Analytical and Numerical Studies of Weakly Nonlocal Solitary Waves of the Rotation-Modified Korteweg-deVries Equation

Guan-yu Chen *

John P. Boyd†

Department of Atmospheric, Oceanic & Space Science
University of Michigan, 2455 Hayward Avenue, Ann Arbor MI 48109
jpboyd@engin.umich.edu;
http://www.engin.umich.edu:/∼ jpboyd/

September 19, 2000

*Permanent address: Institute of Harbour and Marine Technology,Wuchi, Taichung 435, Taiwan

†Corresponding author

Table 1: Rotation-Modified KdV: Select Bibliography

References	Descriptions
Ostrovsky[21]	Derivation for water waves with rotation
Leonov[19]	Nonexistence of classical solitons
Redekopp[23]	Derivation for water waves with rotation
Ostrovsky&Stepanyants[22]	Review with some numerical solutions and extensive bibliography
Hunter[17]	Matched asymptotics: KdV solitons are the "inner" approximation; sinusoidal wave of wavenumber $k_f \sim \epsilon$ is the outer approximation
Galkin&Stepanyants[10]	Nonexistence of classical solitons
Gilman&Grimshaw &Stepanyants[11, 12]	Construct periodic solutions with KdV soliton as "inner" approximation; parabolic arc as "outer"
Grimshaw&He&Ostrovsky[15]	Radiative decay and spontaneous rebirth of weakly nonlocal solitary waves
Grimshaw& Ostrovsky[13] Shrira&Stepanyants	Review of both RMKdV and RMKP solitons and water waves

Abstract

A century ago, the Korteweg-deVries (KdV) equation was derived as a model for weakly nonlinear long waves propagating down a channel when cross-channel and depth variations are sufficiently weak. In this article, we study the steadily-translating coherent structures of a generalization of this equation, the Rotation-Modified Korteweg-deVries equation, which applies when Coriolis forces are significant: $(u_t + uu_x + u_{xxx})_x - \epsilon^2 u = 0$ where x is the down-channel coordinate. (This is also called the "Ostrovsky" equation). The RMKdV solitary waves are weakly nonlocal due to the radiation of long waves where the radiation is proportional to the small parameter ϵ. Because of its simplicity, the RMKdV coherent structures are the prototype of nonlocal solitary waves where the amplitude is a power of the small parameter ("micropterons"). We extend the matched asymptotic expansions of Hunter to third order. We also compute direct numerical solutions and bifurcations of the nonlinear eigenvalue problem. New modes, with multiple KdV-like peaks flanked by small quasi-sinusoidal oscillations, are shown to be well-described by matched asymptotics, too.

PACS Classification Numbers: 4735, 9220, 0340K

Keywords: solitary waves, gravity waves, weakly nonlocal solitons, matched asymptotic expansions

1 Introduction

Rotation-modified gravity waves have been the subject of intense study through laboratory experiments, numerical models and theory. Table 1 is a partial listing. The most sophisticated work allows for cross-channel variations; in this case, the simplified theoretical model is the Rotation-Modified Kadomtsev-Petviashvili (RMKP) equation. When the wave is independent of the cross-

channel coordinate y, then the evolution is described by a simpler wave equation in one space dimension, the Rotation-Modified Korteweg-deVries (RMKdV) Eq. Much remains unknown even for this simpler case, so in this article, we shall restrict ourselves the RMKdV model:

$$\frac{\partial}{\partial x}\left(u_t + uu_x + u_{xxx}\right) - \epsilon^2 u = 0 \qquad \text{RMKdV Eq.} \tag{1}$$

In the Russian literature, this is usually called the "Ostrovsky" equation. Note that this is written in a frame of reference which is moving at the linear long wave speed c_0 where for shallow water waves, $c_0 = \sqrt{gH}$ where H is the mean fluid depth and g is the gravitational constant, $9.8m^2/s$. The small parameter ϵ measures the relative strength of Coriolis forces. The RMKdV equation was derived for water waves by Ostrovsky[21], Redekopp[23] and Grimshaw [14] using singular perturbation theory under the assumption that the water depth is shallow, cross-channel variations are negligible and the amplitude is small.

The steadily-translating solutions of this partial differential equation solve the ODE

$$-cu_{XX} + u_X^2 + uu_{XX} + u_{4X} - \epsilon^2\, u = 0 \qquad \text{[stationary RMKdV]} \tag{2}$$

where $X = x - ct$. The steadily-translating coherent structures fall into two broad categories: weakly nonlocal solitary waves ("micropterons") and spatially periodic solutions ("micropteroidal waves"). The nonlocal solitary waves have only a single large peak on the interval $X \in [-\infty, \infty]$. Hunter[17] has shown through the method of matched asymptotic expansions that Eq.(2) has micropterons of the form (for $c = 1$)

$$u \sim 3\mathrm{sech}^2(X/2) - \,6\,\epsilon\,\left[\sin(\epsilon|X|) + \,\chi\,\cos(\epsilon X)\right], \qquad \epsilon << 1 \tag{3}$$

where χ is an arbitrary constant that is zero for the micropteron of minimum amplitude. The sech-squared peak identical in form to the solitary wave of the usual Korteweg-deVries equation, which is the limit $\epsilon \to 0$ of the RMKdV equation.

The micropteroidal wave is very similar except that the sech-squared peaks are repeated with a spacing equal to the spatial period in X. There is a close relationship between the solitary waves and periodic solution which will be exploited below in the discussion of numerical solutions: one can compute the solitary wave by computing the micropteroidal wave instead because the two closely approximate one another over an interval centered on the sech-squared peak.

The approximation Eq. (3) forces the core of the solitary wave, $3\mathrm{sech}^2(X/2)$, to have a single fixed width. The complete family of solitary waves depends on three parameters, which can be taken to either (c, ϵ, χ) or the some measure of the amplitude plus ϵ and χ. However, the micropterons are only a two-parameter family of shapes, which can be explored in its entirety by fixing c (here, at $c = 1$) and varying only ϵ and χ, because of the following.

Theorem 1 (RESCALING)
Suppose that $v(x; c, \epsilon)$ *is a solution to*

$$-cv_{XX} + v_X^2 + vv_{XX} + v_{4X} - \epsilon^2 v = 0 \tag{4}$$

Then

$$u \equiv \lambda^2 v(\lambda x; c\lambda^2, \lambda^2 \epsilon) \tag{5}$$

is a solution also for arbitrary constant λ.

In the $c - \epsilon$ plane, the rescaling theorem implies the shape of u is invariant, to within rescaling of amplitude and width, everywhere along the line

$$c = \lambda^2 \tilde{c}, \qquad \epsilon = \lambda^2 \tilde{\epsilon} \tag{6}$$

where λ is the parameter of the ray and where the far field parameter χ is assumed fixed.

Previous work on the RMKdV equation has mostly been restricted to proving the non-existence of classical solitary waves, that is, steadily-translating coherent structures whose amplitude decays to *zero* [instead of a sinusoidal oscillation of amplitude $O(\epsilon)$] as $|X| \to \infty$. Ostrovsky&Stepanyants[22], Galkin&Stepanyants[10] and Gilman, Grimshaw and Stepanyants[11, 12] have presented some numerical solutions and constructed periodic approximations. However, this work is dominated by an exact parabolic solution which generates only a subset of the much larger family of solitary and periodic solutions captured by Hunter's [17] matched asymptotic expansion.

Hunter's work, which was never published in a journal, captures both the central, KdV-like core and the sinusoidal "wings" in simple analytic approximations. However, he did not calculate the $O(\epsilon)$ inner approximation or make any comparisons between his theory and numerical computations. In this article, we remedy both these deficiencies and carry his analysis to higher order to show that no inconsistencies or new physics develops at least up to fourth order. We also discuss the numerical difficulties of directly solving a nonlinear eigenvalue problem which contains multiple length scales — the narrow scale of the sech-squared core, the wide scale of the sinusoidal wings — and is resonant for certain discrete spatial periods. We carefully analyze the linear dynamics which applies far from the central core to understand why the central peak is accompanied by small amplitude sinusoidal oscillations that fill all of space. We explain the role of the phase parameter — arbitrary on the infinite interval, controlled by the spatial period when periodic boundary conditions are imposed — and the extremes of minimal radiation and of unbounded amplitude resonance. Lastly, we try to explain the lessons that can be learned from this simple exemplar that are relevant to more complicated species of nonlocal solitary waves.

In our companion article [8], we concentrate on the "quasi-cnoidal" mode, that is, RMKdV waves which have maxima that are all of equal size. In this paper, we focus on waves with both tall, sech-squared-like peaks and small amplitude sinusoidal oscillations.

There has been much study of the FKdV equation

$$\epsilon^2 u_{5X} + u_{XXX} + (u-c)u_X - \epsilon^2\, u = 0 \qquad \text{[stationary RMKdV]} \tag{7}$$

Like our problem Eq. 2, this is a perturbation of the Korteweg-deVries. However, the perturbation is a derivative that *raises the order* of the differential whereas for the RKMKdV equation, the perturbation is of lower order than the KdV terms. As reviewed in the monograph by Boyd [5], this seemingly insignificant difference has a profound significance.

For the FKdV equation, the perturbation creates a *high wavenumber* resonance at a wavenumber k_f which is inversely proportional to ϵ. Because the amplitude of these high wavenumber resonant waves is exponentially small in k, the amplitude of the far field oscillations is *exponentially small* in $1/\epsilon$.

In contrast, the nonlocal-generating-resonance is a *long wave* resonance with the resonant wavenumber $k_f \sim O(\epsilon)$. The far field oscillations, as first shown by Hunter, are then $O(\epsilon)$. The special tools of exponential asymptotics, so essential for the FKdV equation, are unnecessary. By this same token, the theory of the FKdV equation is of rather limited value in understanding the RMKdV equation.

2 Far Field Analysis and the Linear Dispersion Relation

Far from the core of the soliton where the amplitude is small — if it is truly "weakly" nonlocal, one can neglect all the nonlinear terms to obtain

$$-cu_{XX} + u_{4X} - \epsilon^2\, u \approx 0 \qquad\qquad |X| >> 1 \tag{8}$$

This has sinusoidal solutions proportional to $\exp(ikX)$ if the wavenumber satisfies the dispersion relation

$$c_{linear}(k) = -\,k^2 + \frac{\epsilon^2}{k^2} \tag{9}$$

The far field oscillations have a wavenumber k_f such that $c_{linear}(k_f) = c_{soliton}$. With Hunter's convention of specializing to solitary waves of unit phase speed, this implies

$$k_f \sim \epsilon \tag{10}$$

to lowest order as illustrated in Fig. 1.

The group velocity is

$$c_g = \frac{\partial \omega}{\partial k} = -3\,k^2 - \frac{\epsilon^2}{k^2} \tag{11}$$

In the limit $k \to 0$, the group velocity is infinite! This is not a serious difficulty because of the following.

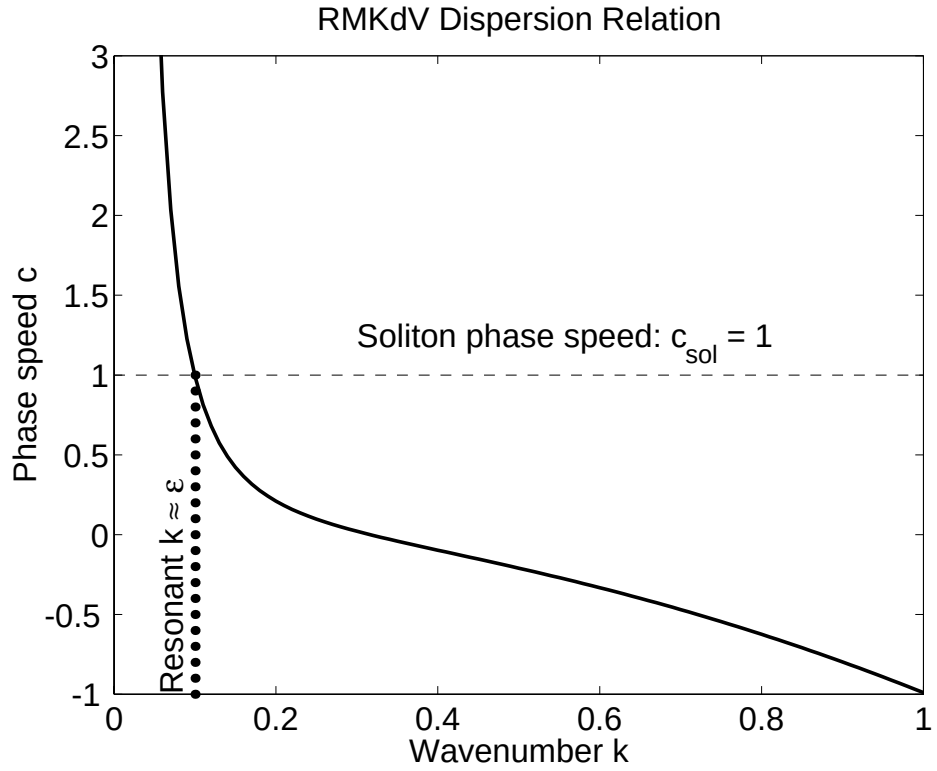

Figure 1: The heavy solid line is the *linear* dispersion relation for sine waves of wavenumber k for the RMKdV equation. Resonance occurs when the phase speed $c(k)$ matches that of the soliton. Here, $c_{sol} = 1$ (thin, dashed horizontal line). Resonance occurs for $k \approx \epsilon$ as marked by the dotted line. Slightly modified from Fig. 15.2 of [5], published by Kluwer.

Theorem 2 (ZERO MEAN)
If $u(X)$, a solution to the RMKdV equation, satisfies periodic boundary conditions with spatial period P, then (including the limit $P = \infty$)

$$\int_{-P/2}^{P/2} u dx = 0 \tag{12}$$

The first step of the proof is to integrate the partial differential equation with respect to x. Since all terms except that multiplied by ϵ are x-derivatives, the result of integrating them and applying the periodic boundary condition is zero. [1]

[1]The RMKdV equation has several additional conservation laws in addition to the constraint of zero mean as catalogued by Grimshaw, Ostrovsky, Shrira and Stepanyants[13] and Benilov[2], but we shall not need them here.

Therefore, wavenumber $k = 0$ is always missing from the Fourier series or Fourier transform of any solution. One can show by explicit integration that both Hunter's approximation[17] and also that of Gilman, Grimshaw and Stepanyants[11, 12] satisfy the zero mean constraint for all combinations of the parameters.

When the time-dependent RMKdV is solved using a spatially localized initial condition, the core will radiate waves of wavenumber $k_f \approx \epsilon$ [15]. The group velocity of these waves, which determines the speed with which the wave packet will spread away from the core, is simply

$$c_g(k_f) \approx -1 \tag{13}$$

Since the soliton itself is moving at unit speed to the right, the radiated waves will always trail the soliton to the left with the trailing edge of the wave disturbance propagating at a speed of -2 relative to the core of the disturbance.

3 Symmetry and Antisymmetry

A function is said to be "symmetric" with respect to $X = 0$ if $u(X) = u(-X)$ and "antisymmetric" if $u(X) = -u(-X)$. In later sections, we shall assume that the solution is symmetric. No unsymmetric solutions are known (except for the trivial exception noted below), but an open problem is to prove that all solutions are symmetric.

We have proved the following partial result:

Theorem 3 (NONEXISTENCE of ANTISYMMETRIC SOLUTIONS) *Steadily-translating solutions which are purely antisymmetric, that is,*

$$u(X - X_0) = -u(-[X - X_0]) \tag{14}$$

for some point of antisymmetry X_0, are impossible for the RMKdV equation.

PROOF: A general function $u(X)$ can always be decomposed into its symmetric and antisymmetric parts[4]. Let

$$u = S(X) + A(X) \tag{15}$$

where S and A are its symmetric and antisymmetric parts, respectively. For notational simplicity, we set the symmetry point $X_0 = 0$, but since the differential equation is translationally invariant, the argument is general, and applies for arbitrary X_0. Note that differentiation reverses parity so that the first derivative of a symmetric function is antisymmetric and so on. The stationary RMKdV equation can be split into a coupled system of two equations in which all terms in one member of the set are symmetric and another in which all terms are antisymmetric:

$$-cS_{XX} + S_{4X} - \epsilon^2 S + S_X^2 + A_X^2 + SS_{XX} + AA_{XX} = 0 \tag{16}$$

$$-cA_{XX} + A_{4X} - \epsilon^2 A + 2S_X A_X + SA_{XX} + S_{XX}A = 0 \tag{17}$$

For a purely antisymmetric solution, $S(X) \equiv 0$. The first equation then reduces to

$$(AA_X)_X = 0 \tag{18}$$

whose general solution, $A(X) = \pm\sqrt{\alpha X + \beta}$, is not antisymmetric for any choice of the arbitrary constants α and β. Q. E. D.

Unfortunately, it is not easy to rule out solutions which are a mixture of symmetric and antisymmetric components. Because the RMKdV is translationally invariant, that is, has coefficients which have no explicit dependence on X, it follows that if $u(X)$ is a solution, then its translation $u(X + \phi)$ is also a solution for some arbitrary ϕ. If $u(X)$ is symmetric, then its translate $u(X + \phi)$ will be a *mixture* of symmetric and antisymmetric components. It follows that when we speak of a "symmetric" solution, we mean a solution that can be made symmetric by a translation.

One intriguing feature of the antisymmetric equation, Eq. 17, is that it is *linear* in $A(X)$. The antisymmetric part of a solution must therefore be an eigenfunction with zero eigenvalue of a linear eigenproblem with coefficients that depend on $S(X)$. (This is true not only of the RMKdV equation, but of any ODE with a quadratic nonlinearity.) The derivative of a symmetric solution, $A(X) \equiv S_X$, is always and automatically such an eigensolution so that the translation of a symmetric solution by an arbitrarily small shift ϕ is a solution, too. The unmet challenge is to prove the existence or nonexistence of other species of antisymmetric eigenfunctions.

4 Matched Asymptotics: Overview

As noted in the introduction, in the rest of the article we assume without loss of generality that (i) the phase speed of the nonlocal solitary wave is $c = 1$ and (ii) the sech-squared-like peak [core] has been centered at $X = 0$ in the moving reference frame. As shown in the previous section, the length scale of the small amplitude sinusoidal oscillations is $O(1/\epsilon)$ whereas that of the core is $O(1)$. Hunter[17] showed that because of this separation of length scales and also because the core is well-approximated, for small ϵ, by the KdV solitary wave whereas the wings are well-approximated by a cosine function, it is possible to systematically approximate the nonlocal solitary wave everywhere by using the method of matched asymptotic expansions.

Fig. 2 shows the "inner" and "outer" regions. The coherent structure will be approximated by different expansions, using different rescaled spatial coordinates, in each region. The two series will then be matched, term-by-term, in the overlap region where both approximations are legitimate to obtain a global approximation. The "inner coordinate" is X; the slow, "outer" coordinate is

$$\xi \equiv \epsilon\, X \qquad \text{Outer coordinate} \tag{19}$$

The following points will be elaborated below.

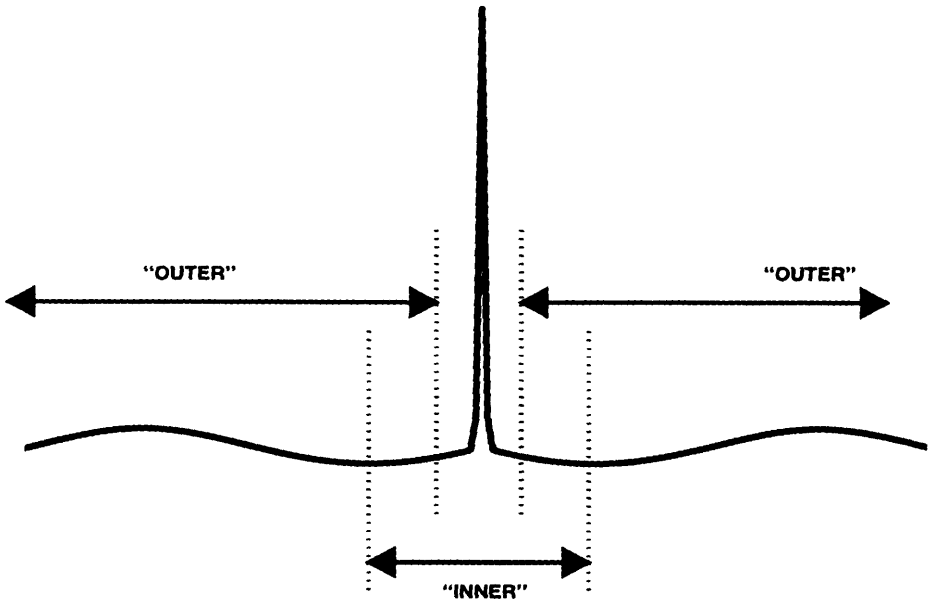

Figure 2: Schematic of the inner and outer regions for the matched asymptotic expansion of the RMKdV nonlocal solitary wave for $\epsilon << 1$. The two approximations are matched in the overlap region where both the inner and outer approximations are *simultaneously* accurate as $\epsilon \to 0$. The length scale of the inner region is $O(1)$; the length scale of the outer region is $O(1/\epsilon)$.

- The outer solution is a sine wave altered by smaller higher harmonics.
- At each order, the outer solution is approximated by a trigonometric polynomial whose degree increases as the order in ϵ increases.
- The first and second orders of the "inner" solution are given here for the first time, and as explicit, exact analytical expressions.
- The third and higher inner orders cannot be given in simple, analytical form, but can be computed numerically using special spectral methods.
- The outer limit of the inner solution, that is, the large-$|X|$ asymptotic form of the inner solution, is a polynomial in X whose degree is one less than the order, that is, u_0 decays exponentially, u_1 asymptotes to a constant, u_2 asymptotes to a linear polynomial of X and so on.
- Because the outer limit is *unbounded*, the usual spectral basis for an unbounded domain must be augmented with special basis functions.
- The inner limit of the outer solution also takes the form of a polynomial in X. Matching is thus straightforward; no logarithms in ϵ arise.

- Comparisons with numerical solutions show that the perturbative approximations are quite accurate even for moderately large ϵ.

4.1 Mechanics of Matching

Define the outer variable

$$\xi = \epsilon X \tag{20}$$

Let I_n denote the result of truncating the asymptotic series for *fixed inner variable* X up to and including the $O(\epsilon^n)$ term [so that the error in $I_n(u)$ is proportional to ϵ^{n+1}]. Let O_m denote the result of truncating the series for *fixed outer variable* ξ up to and including the m-th term.

Let $u^{(outer)}(\xi, \epsilon)$ denote the outer expansion and $u^{(inner)}(X, \epsilon)$ denote the inner expansion. Van Dyke's Matching Principle is

$$O_n I_m u^{(inner)} = I_m O_n u^{(outer)} \tag{21}$$

Although discovered earlier by Lagerstrom, Kaplun and others, the matching formalism was stated most lucidly by Van Dyke(1975)[24] and so the matching rule is commonly labelled with his name.

In this notation,

$$I_m u^{(inner)} = \sum_{j=0}^{m} \epsilon^j \, u_j(X) \, . \tag{22}$$

To take the outer limit, we must replace each u_j by its large X approximation:

$$I_m u^{(inner)} \sim \sum_{j=1}^{m} \sum_{k=0}^{j-1} p_{jk} \epsilon^j |X|^k \, . \tag{23}$$

Note that lower index on the sum in j has been changed to one because u_0 decays exponentially with $|X|$ and therefore does not contribute to the asymptotic matching.

Next, rewrite the inner series in terms of the outer coordinate:

$$\begin{aligned} I_m u^{(inner)} &= \sum_{j=1}^{m} \sum_{k=0}^{j-1} p_{jk} \epsilon^{j-k} |\xi|^k \\ &= \sum_{j=1}^{m} \epsilon^j \sum_{k=0}^{m-j} p_{j+k,k} \, |\xi|^k \end{aligned} \tag{24}$$

where we have rearranged the sum in the second line so as to extract powers of ϵ. The outer limit O_n is just the truncation of the second sum at $O(\epsilon^n)$:

$$O_n I_m u^{(inner)} = \sum_{j=1}^{n} \epsilon^j \sum_{k=0}^{m-j} p_{j+k,k} \, |\xi|^k \tag{25}$$

Similarly, the first step in deriving the inner limit of the outer solution is to expand the outer solution for small coordinate ξ:

$$O_n u^{(outer)} \approx \sum_{J=1}^{n} \epsilon^J \sum_{K=0}^{\infty} q_{JK}\, \xi^K \tag{26}$$

The inner limit is obtained by replacing $\xi \to \epsilon X$ and then reexpanding in powers of ϵ and X.

These matching conditions can be summarized, to all orders, by the analytic formula

$$p_{jk} = q_{j-k,k} \tag{27}$$

for all j, k which are included in the $O_m(I_n)$ limit. It is convenient to catalogue the lowest few instances in Table 2.

The frame-boxes in the table indicate the unknowns which are determined by each matching condition. The unknowns b_1, b_{21}, b_{31}, etc., are the coefficients of the expansion in powers of ϵ of the amplitude of $\sin(kX)$, the fundamental, in the outer solution. Aside from the phase factor χ, which is a free parameter on the infinite interval and is determined by the spatial period P when periodic boundary conditions are imposed, the amplitude of the fundamental completely determines the outer solution. The unknowns $\Lambda_1, \Lambda_2, \Lambda_3$, etc., are constants of integration in the inner solution. The matching constraints labeled "Redundant" are automatically enforced by lower order matches, and thus do not allow us to solve for an unknown.

It is important to note that the matching depends only on the coefficients p_{jk} and q_{jk} of the power series which are the outer limit of the inner solution and the inner limit of the outer solution. It follows that only the asymptotic-in-space inner and outer solutions are needed for the match. Hunter, for example, was unable to explicitly determine the inner solution at second order. He nevertheless successfully matched the *asymptotic* (large X) second order inner solution to the first order outer solution to obtain a complete lowest order solution for all X. [2]

4.2 Explicit Example of Matching

To illustrate the abstract and symbolic matching conditions described above, consider the same order as in Hunter's work: the $m = 2, n = 1$ match, i. e.,

$$I_2 u^{(inner)} \epsilon \left\{ p_{10} + p_{21} |\xi| \right\} + \epsilon^2 p_{20} \tag{28}$$

The first order outer limit of the second order inner solution is

$$\begin{aligned} O_1 I_2 u^{(inner)} &= \epsilon p_{10} + \epsilon^2 p_{21} X \\ &= -\Lambda_1 \epsilon - 6\epsilon^2 X \end{aligned} \tag{29}$$

[2] Hunter's result is not a proper composite expansion because the inner solution is known only at $O(1)$ and not at $O(\epsilon)$, which is the magnitude of the outer solution. A second order composite solution is given here for the first time, exploiting our analytic solutions for the first and second order inner equations.

Table 2: Matching Constraints

j k	0	1	2	3
1	$p_{10} = q_{10}$ $\boxed{\Lambda_1}$			
2	$p_{20} = q_{20}$ $\boxed{\Lambda_2}$	$p_{21} = q_{11}$ $\boxed{b_1}$		
3	$p_{30} = q_{30}$ $\boxed{\Lambda_3}$	$p_{31} = q_{21}$ $\boxed{b_{21}}$	$p_{32} = q_{12}$ [REDUNDANT]	
4	$p_{40} = q_{40}$	$p_{41} = q_{31}$ $\boxed{b_{31}}$	$p_{42} = q_{22}$ [REDUNDANT]	$p_{43} = q_{13}$ [REDUNDANT]

The outer solution to this order is

$$O_1 u^{(outer)} = \epsilon \left\{ a_1 \cos(\epsilon X) + b_1 \sin(\epsilon X) \right\}. \tag{30}$$

If we expand in powers of ϵ for fixed inner variable and truncate by discarding $O(\epsilon^3)$, we obtain

$$I_2 O_1 u^{(outer)} = a_1 \epsilon + b_1 \epsilon^2 X \,. \tag{31}$$

The Matching Principle gives

$$\begin{aligned} I_2 O_1 u^{(outer)} &= O_1 I_2 u^{(inner)} \\ a_1 \epsilon + b_1 \epsilon^2 X &= -\Lambda_1 \epsilon - 6\epsilon^2 X \end{aligned} \tag{32}$$

This implies

$$a_1 = -\Lambda_1, \qquad b_1 = -6 \tag{33}$$

5 Inner Solution

The inner solution is expanded as

$$u(X;\epsilon) \sim u_0(X) + \epsilon u_1(X) + \epsilon^2 u_2(X) + \ldots \tag{34}$$

where

$$u_0 \equiv 3\mathrm{sech}^2(X/2) \tag{35}$$

(The phase speed is chosen to be $c = 1$; recall that solutions for other phase speeds can be found from that for unit phase speed by applying the Rescaling Theorem above.)

It is convenient to integrate the perturbative equations twice with respect to X so as to convert them into second order equations, which are easier to solve.

The first and second order solutions were computed by making the "tanh" transformation described in the next subsection.

Table 3: Equivalents Under the Tanh Transformation

z	X
z	$\tanh(X/2)$
$1-z^2$	$\mathrm{sech}^2(X/2)$
$\frac{1}{1-z^2}$	$\cosh^2(X/2),\ 1+\sinh^2(X/2)$
$\frac{z}{\sqrt{1-z^2}}$	$\sinh(X/2)$
$\log(1-z^2)$	$-2\log(\cosh(X/2))$
$\log\left\{\frac{1-z}{1+z}\right\}$	$-X$
$-\frac{1}{2}\log(1-z^2)$	$\log(\cosh(X/2))$
$\frac{1}{2}(1-z^2)\frac{d}{dz}$	$\frac{d}{dX}$
$\int_{\tanh(a/2)}^{\tanh(b/2)} 2\frac{f(2\mathrm{arctanh}(z))}{1-z^2}dz$	$\int_a^b f(X)dX$
$\frac{1}{4}(1-z^2)\left\{(1-z^2)\frac{d^2}{dz^2}-2z\frac{d}{dz}\right\}$	$\frac{d^2}{dX^2}$
$\{(1-z^2)u_{zz}-2zu_z\}-\frac{\mu^2}{1-z^2}u+\nu(\nu+1)u=4\frac{f(2\mathrm{arctanh}(z))}{1-z^2}$	$u_{XX}+\left\{\frac{\nu(\nu+1)}{4}\mathrm{sech}^2(X/2)-\frac{\mu^2}{4}\right\}u=f(X)$

Note: The differential operator in z in the last line is the usual Legendre differential equation; its homogeneous solutions are $P_\nu^\mu(z), Q_\nu^\mu(z)$.

5.1 Tanh Transformation

Symbolic manipulation language systems such as Maple and Mathematica are much better at manipulating *polynomials* than *transcendentals*. The transformation $z=\tanh(X/2)$ is helpful because the perturbative equations have only *polynomial* coefficients when transformed to the new coordinate z (Appendix B of [5]). Through its built-in symbolic ordinary differential solver ("**dsolve**"), the symbolic language Maple then yielded, explicit, analytic solutions to both the first and second order inner problems which are given here for the first time. (Hunter[17] solved these problems only in the *asymptotic* limit $|X|\to\infty$.)

Table 3 collects the various identities which are helpful in transforming to the new coordinate z and then back again.

Unfortunately, it was not possible to find complete explicit inner solutions at third and higher order.

5.2 First Order Inner Solution

The inner problem at first order is

$$u_{1,XX}+(u_0(X)-1)u_1=\Lambda_1 \tag{36}$$

where Λ_1 is constants of integration that will be determined by matching. We have implicitly suppressed one constant of integration for each equation by assuming that $u(X)$ is a symmetric function of X. Both the analysis and numerics confirm that such symmetric solutions exist; the question of possible asymmetric solutions is still open.

Hunter[17] solved the first and second order inner approximations only in the limit $|X| \to \infty$. This was sufficient for matching the inner and outer solutions, but not for forming a composite expansion which is uniformly accurate for all X. We find that, without approximation,

$$u_1 = \Lambda_1 \mathcal{E}; \qquad \mathcal{E} \equiv -1 + 3\mathrm{sech}^2(X/2)\,\{1 - (X/2)\tanh(X/2)\} \tag{37}$$

The first order solution is plotted in Fig. 3.

One subtlety is that in its original, fourth order form, the first order perturbative equation is *homogeneous*. It follows that u_1 is an exact *eigenfunction* of the differential operator $\mathcal{L}$ which is common to the perturbative equations of all orders when these are written in their un-integrated, fourth order form where

$$\mathcal{L} \equiv \frac{d^4}{dX^4} + (u_0 \, - \, 1\,)\frac{d^2}{dX^2} + u_{0,XX} + 2u_{0,X}\frac{d}{dX} \tag{38}$$

When $\mathcal{L}$ is integrated twice, the implicit degree of freedom created by this eigenfunction of zero eigenvalue becomes explicit as the constant of integration Λ_j at j-th order. Part of u_j will therefore be $\Lambda_j \mathcal{E}$ where the normalized eigenfuction $\mathcal{E}$ is defined by Eq. 37 above.

The reason that the perturbative equation at first order is homogeneous (except for Λ_1) is that the ϵ-dependent term in the RMKdV equation is proportional to ϵ^2, and therefore appears only at second and higher order. In the far field, the wavenumber of the quasi-sinusoidal outer solution is approximately ϵ, rather than its square as appears in the differential equation. This dependence of the first power of ϵ in the outer solution can induce a similar dependence on the inner solution through matching.

For large X, as needed to take the outer limit of the inner solution,

$$u_1 \sim -\Lambda_1, \qquad |X| >> 1 \tag{39}$$

as follows from the limits

$$\lim_{X\to\infty} \mathrm{sech}(X) = 0, \qquad \lim_{X\to\infty} \tanh(X) = \mathrm{sign}(X) \tag{40}$$

This implies that the coefficients of the power series in X for large X have

$$p_{10} = -\Lambda_1, \qquad p_{1j} = 0, \qquad \forall j > 0 \tag{41}$$

5.3 Second Order Inner Approximation

The second order perturbative equation is

$$\begin{aligned} u_{2,XX} + (u_0(X) - 1)u_2 &= \Lambda_2 + \int_0^X \int_0^\eta u_0(\zeta) d\zeta\, d\eta - \frac{1}{2}u_1^2 \\ &= \Lambda_2 + 12\,\log(\cosh(X/2)) - \frac{1}{2}\Lambda_1^2\,\mathcal{E}^2 \end{aligned} \tag{42}$$

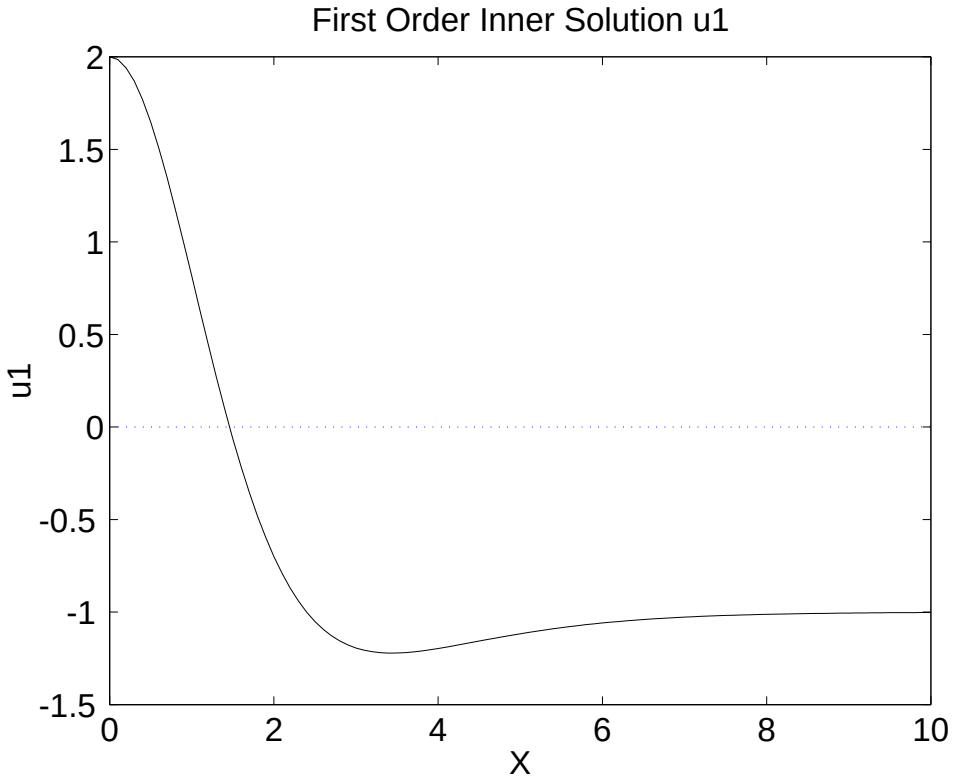

Figure 3: A graph of $\mathcal{E}$, which is u_1/Λ_1. Note that it asymptotes to the constant -1. To lowest order in ϵ, the integration constant Λ_1 (and therefore the first order solution) turn out to be zero for a "minimum" radiation solution, that is, when the outer solution is as small as possible for a given ϵ.

where Λ_2 is again an integration constant which will be determined by matching. As noted earlier, this equation was solved by making the "tanh" transformation, invoking the Maple differential equation solver, and then converting the result back to the original coordinate. The Maple solution is not symmetric with $X = 0$ as it should be, but can be made so by adding an appropriate multiple of the eigensolution $\mathcal{E}$; similarly, replacing expressions like $\log(z-1) + i\pi$ by $\log(1-z)$ was tedious but elementary.

Define

$$y \equiv X/2, \qquad \text{sh} \equiv \text{sech}(X/2), \qquad \text{th} \equiv \tanh(X/2) \tag{43}$$

and denote the so-called "dilogarithm" function by "dilog"; the solution is

$$u_2 = u_{2a} + \Lambda_1^2\, u_{2b} + \Lambda_2\, \mathcal{E} \tag{44}$$

$$
\begin{aligned}
u_{2a} \;=\;& 12\mathrm{sh}^2 + 24\log(\cosh(y)) - 36\mathrm{th}^2\,\log(\cosh(y)) - 18\,y\,\mathrm{th}\,\mathrm{sh}^2\,\log(\cosh(y)) \\
& + \{18\log(2) - 48\}\,y\,\mathrm{th}\,\mathrm{sh}^2 \\
& + 9\mathrm{th}\,\mathrm{sh}^2\,\{\mathrm{dilog}(1/2 + \mathrm{th}/2) - \mathrm{dilog}(1/2 - \mathrm{th}/2)\}
\end{aligned} \tag{45}
$$

$$
u_{2b} = -1 + \frac{3}{2}\,\mathrm{th}^2 - \frac{3}{4}y\;(\mathrm{th} + y)\;\mathrm{sh}^2 + \frac{9}{4}\,y^2\,\mathrm{th}^2\,\mathrm{sh}^2 \tag{46}
$$

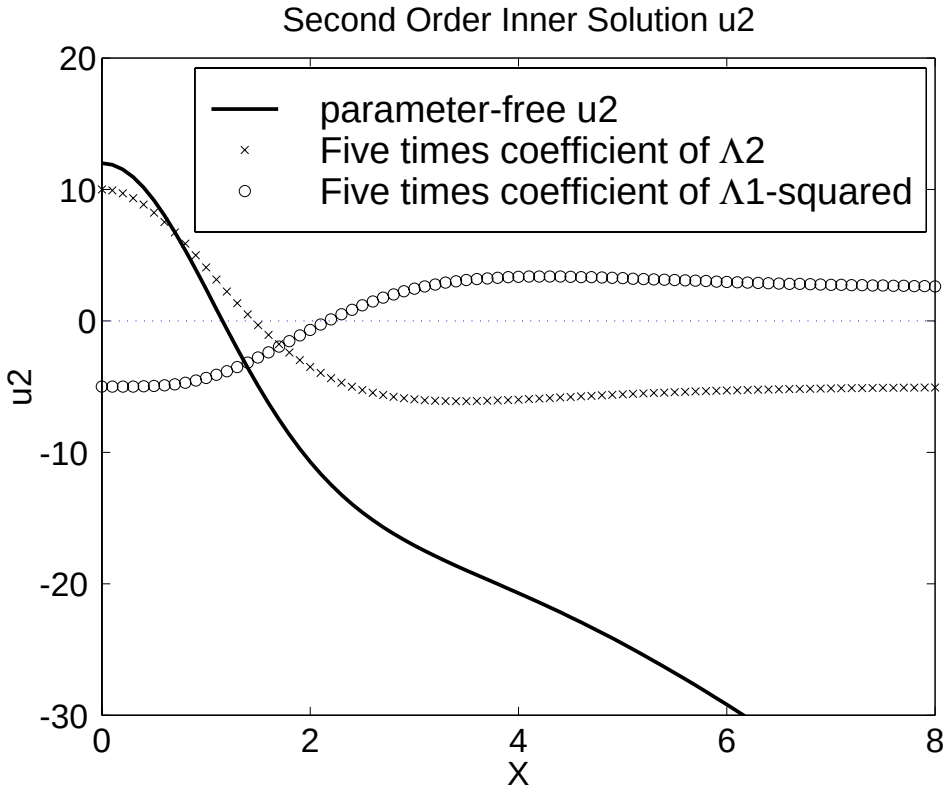

Figure 4: A graph of the three parts of u_2. The heavy solid curve shows u_{2a}, which is that part of u_2 which is not multiplied by a constant of integration, and is therefore *independent* of the outer solution. This is large compared to the coefficients of the integration constants Λ_2 (circles; $\mathcal{E}$) and Λ_1^2 (x's; u_{2b}), and asymptotes to a *linear* function of X. In contrast, the other two parts, which are shown multiplied by a factor of 5, asymptote to *constants* as $|X| \to \infty$. The graph of the coefficient of Λ_2 is identical, except for multiplication by five, to the first order solution graphed in the previous figure.

Table 4: Matlab Code for the Dilogarithm

```
function f=dilog(x);
% Evaluates dilog(x) = - ∫_1^x dt log(t)/(t-1), x ∈ [0,∞]. Reference: pg. 1004
% NBS Handbook of Mathematical Functions,Abramowitz & Stegun (1965)
if x==0, f=pi*pi/6;
elseif (x>0) & (x < 1/2), f = -dilog_aux(1-x)-log(x)*log(1-x)+pi*pi/6;
elseif (x >= 1/2) & (x <= 1), f = dilog_aux(x); end
```

```
function f=dilog_aux(x);
% Evaluates the dilog function by power series for x ∈ [1/2,1]
f=0; for k=1:50, f = f +((-1)* (x-1))^k / (k*k); end
```

The second order solution has three parts. The first part u_{2a}, which is completely independent of the integration constants, Λ_1 and Λ_2, is forced by the double integral of the $-\epsilon^2 u_0$. The second part, proportional to Λ_1^2, arises from the nonlinear interaction of the first order solution with itself. The third part, proportional to Λ_2, is the linear eigenfunction $\mathcal{E}$ of zero eigenvalue of the perturbative differential operator; this is identical in form to u_1 except for the replacement of $\Lambda_1 \to \Lambda_2$. All three parts (with scaling) are graphed in Fig. 4.

It appears that no explicit analytic solutions exist for higher order; the second order solution already involves an unfamiliar transcendental, the dilogarithm[20] ("Spence's integral"). This function is defined by, as on pg. 1004 of [1],

$$\mathrm{dilog}(z) \equiv -\int_1^z \frac{\log(t)}{t-1}\,dt \tag{47}$$

Although this function cannot be written as an exact, finite sum of simpler functions, it is nevertheless easy to evaluate numerically for the relevant interval $x \in [0,1]$ as illustrated by the short Matlab code, Table 4. It is also easy to write down high accuracy approximation for that part of u_{2a} which is multipled by the dilogarithm. For example,

$$\begin{aligned} &\Big|\ 9\,\mathrm{th}\,\mathrm{sh}^2(\mathrm{dilog}(1/2+\mathrm{th}/2)-\mathrm{dilog}(1/2-\mathrm{th}/2)) \\ &-9\,\mathrm{th}^2\,\mathrm{sh}^2\left\{-1.36-0.223\,\mathrm{th}^2)\right\}\Big| \le 0.042\ \forall\, X \end{aligned} \tag{48}$$

where the approximation minimizes the maximum pointwise error for formulas of the indicated form. The maximum absolute error is only 1/1180 of the total range in Fig. 4.

In the outer limit, that is, $|X| >> 1$, the second order problem simplifies to

$$u_{2,XX} - u_2 \sim 6\,|X| + \left\{\Lambda_2 - 12\log(2) - (1/2)\,\Lambda_1^2\right\} \tag{49}$$

where we have neglected only terms that decay exponentially with $|X|$. The asymptotic approximation, like the right-hand side, is a linear polynomial in X:

$$u_2 \sim -6\,|X| - \left\{\Lambda_2 - 12\log(2) - (1/2)\,\Lambda_1^2\right\} \qquad |X| >> 1 \tag{50}$$

as follows from

$$\log(\cosh(X/2)) = (1/2)|X| - \log(2) \qquad |X| \to \infty\,. \tag{51}$$

This implies that the coefficients of the power series in X for large X have

$$p_{20} = -\left\{\Lambda_2 - 12\log(2) - (1/2)\,\Lambda_1^2\right\},\ \ p_{21} = -6,\ \ p_{2j} = 0, \qquad \forall j > 1. \tag{52}$$

6 Third Order Inner Problem

The differential equation is

$$\begin{aligned} u_{3,XX} + (u_0 - 1)u_3 &= \Lambda_3 + \int_0^X d\theta \int_0^\theta u_1(\eta)d\eta - u_1 u_2 \\ &= \Lambda_3 + \Lambda_1\left\{-\frac{1}{2}X\left\{X\ -\ 6\tanh(X/2)\right\}\right\} - u_1 u_2 \end{aligned} \tag{53}$$

where we have used

$$\int_0^X d\theta \int_0^\theta u_1(\eta)\,d\eta = \Lambda_1\left\{-\frac{1}{2}X\left\{X\ -\ 6\tanh(X/2)\right\}\right\} \tag{54}$$

For large X, the third order equation in the far field becomes

$$\begin{aligned} u_{3,XX} - u_3 \ \sim\ & \Lambda_3\ -\Lambda_1\left\{\Lambda_2 - 12\log(2) - (1/2)\Lambda_1^2\right\} - 3\Lambda_1 X - \frac{\Lambda_1}{2}X^2 \\ & +\text{terms exponentially small in } X \end{aligned} \tag{55}$$

$$u_3 \sim\ -\Lambda_3\ +\ \Lambda_1\left\{\Lambda_2 - 12\log(2) - (1/2)\Lambda_1^2 + 1\right\} + 3\Lambda_1 X + \frac{\Lambda_1}{2}X^2 \tag{56}$$

for large positive X; u_3 for large negative X is obtained by invoking the exact symmetry $u_3(X) = u_3(-X)$, which applies for all X. This asymptotic solution implies, with $p_{3j} = 0$, $\forall j > 2$,

$$p_{30} = -\Lambda_3 + \Lambda_1\left\{\Lambda_2 - 12\log(2) - \frac{1}{2}\Lambda_1^2 + 1\right\}, \qquad p_{31} = 3\,\Lambda_1, \qquad p_{32} = \frac{1}{2}\,\Lambda_1 \tag{57}$$

Obtaining the *complete* solution to the third order problem is much harder. First, when we replace u_2 on the right-hand side by its three parts, the third order problem becomes

$$\begin{aligned} u_{3,XX} + (u_0 - 1)u_3 &= \Lambda_3 + \Lambda_1\left\{-\frac{1}{2}X\left\{X\ -\ 6\tanh(X/2)\right\}\right\} \\ &\quad -\Lambda_1\mathcal{E}(X)\,u_{2a}(X) - \Lambda_1^3\,\mathcal{E}(X)\,u_{2b}(X) - \Lambda_1\Lambda_2\,\mathcal{E}^2(X) \end{aligned} \tag{58}$$

The bad news is that each of the five terms on the right-hand gives rise to a separate subproblem, all differential equations with the same differential operator but different inhomogeneous terms. The good news is that each subproblem can be solved independently of the as-yet unknown integration constants Λ_j, which will be determined later by the phase or spatial period condition imposed on the outer solution, and then the solution multiplied by the appropriate factor of Λ_j's to obtain its contribution to u_3. The very bad news is that not all of these subproblems can be solved in explicit analytical form. The function $u_{2a}(X)$ contains the dilogarithm function, and we have not been able to analytically solve the subproblem where u_{2a} is the inhomogeneous term in the differential equation.

It is possible to *approximately* solve the third and higher order equations by either of two routes. The analytical approach is to replace the dilogarithm by the approximation (48). Maple or Mathematica should then yield an explicit solution, albeit a very complicated one.

The second strategy is numerical. A key point is that the solution to a subproblem such as

$$u_{3a,XX} + (u_0 - 1)u_{3a} = \mathcal{E}(X)\, u_{2a}(X) \tag{59}$$

is *free of parameters*, it needs to be solved numerically just once. The general solution for u_3 will then be a sum of five universal functions of X, each weighted by the appropriate factor of the integration constants Λ_j.

One complication is that the inhomogeneous terms for some subproblems are *unbounded* as $X \to \infty$. We have developed special spectral methods precisely for these sort of problems: a differential equation on a spatially unbounded interval where the solution (and inhomogeneous term) grow as a polynomial in X[7]. Because there are four separate subproblems (plus the coefficient of Λ_3, which is just the eigenfunction $\mathcal{E}$ already found analytically), we shall omit the details here. All these subproblems and their spectral solutions are given with different notation in Chen's thesis (1998)[9].

The important point is that in principle, we can extend the inner solution to any order by using special numerical algorithms and summing an increasing number of parameter-free functions at each order. At fourth order, it is not possible to even obtain the complete large X solution analytically. However, there are no signs of logarithms or a breakdown of the perturbation scheme that would suggest new physics, at least up to and including fourth order.

6.1 Fourth Order Inner Solution

$$u_{4,XX} + (u_0 - 1)u_4 \quad = \quad \Lambda_4 - \frac{1}{2}u_2^2 - u_1 u_3 + \int_0^X d\theta \int_0^\theta u_2(\eta)\, d\eta \tag{60}$$

Although we do not have a complete solution for u_3 nor know the analytical form of the integral of u_2, it is possible to infer at least part of the *asymptotic* solution for u_4.

The contributions of the un-integrated terms in Eq. 60 are obtained by substituting the asymptotic [large X] approximations to u_1, u_2 and u_3 and collecting powers of X. (Note that the *asymptotic* form of u_3 has been explicitly derived in the previous subsection even though the exact third order inner solution is not known, and probably cannot be expressed in terms of elementary functions.)

The double integral of u_2 can be split into its three parts, one proportional to Λ_2, one proportional to Λ_1^2, and one free of parameters, and then each can be numerically integrated using the special, spectrally accurate methods of [7] for single and double integrals of integrands with polynomial growth.

Once the forcing for the fourth order problem is known as a polynomial in X, it is trivial to solve the differential equation, which has constant coefficients for large X, to obtain the polynomial in X which is the large X behavior of u_4:

$$\begin{aligned} u_4 \quad \sim \quad & |X|^3 + \left\{18 + \Lambda_2/2 - 6\log(2) - (3/4)\Lambda_1^2\right\} X^2 \\ & + \left\{3\Lambda_2 - \frac{15}{4}\Lambda_1^2 - 72\log(2) + 28.8229\right\} X + \text{lower order} \end{aligned} \tag{61}$$

7 Outer Solution

7.1 Overview: Stokes Expansions and All That

The outer solution is a Fourier series in which the higher harmonics are expanded in powers of the amplitude a of the lowest order wave, $\cos(kX+\phi)$. $X \equiv x-ct$ as before, c is the phase speed, the spatial period of the outer solution is $2\pi/k$, and ϕ is a constant, the phase factor. Stokes showed in 1847 that weakly nonlinear, spatially periodic water waves could be approximated by such powers-of-the-amplitude Fourier series. Similar series were used forty years later in celestial mechanics as "Poincaré-Lindstedt" expansions.

Whatever the name, the Stokes series has a rather peculiar dual role in the theory of the steadily-translating solutions of the RMKdV equation. First, the Stokes series describes spatially-periodic solutions in which all the crests of the wave are equally tall, and continue indefinitely with even spacing over all of $x \in [-\infty, \infty]$. These solutions are the theme of our companion paper[8].

In addition, the Stokes series also furnishes an outer approximation to the generalized solitary waves of the RMKdV equation in which the small amplitude, quasi-sinusoidal oscillations that fill most of the space are punctuated by an $O(1)$ peak of sech-squared shape, which is the inner solution. In this case, the amplitude of the lowest harmonic is $a \sim O(\epsilon)$. This is a simplification because the solution at n-th order in ϵ is then a trigonometric polynomial of degree n (that is, includes up to and including the n-th harmonics). However, both the amplitude and phase must be adjusted as functions of ϵ at each order so that the outer solution will match smoothly onto the inner.

The Stokes expansion can be written as a *cosine* series with suitable choice of the phase parameter ϕ, but we found it more convenient, in order to avoid arcsines and arctangents of ϕ, to write the solution as a general Fourier series. The ratio of the sine to the cosine coefficient for the fundamental (i. e., $\cos(jkX)$

for $j = 1$) must be the same at higher orders as at first order; the forced harmonics will automatically have the correct phase.

In other applications[3, 16], it is customary to fix the wavenumber k and expand the phase speed. We will make the alternative choice of fixing $c = 1$ and writing

$$k \sim \epsilon \left\{ 1 + \kappa_2 \epsilon^2 + \kappa_3 \epsilon^3 + \kappa_4 \epsilon^4 + \dots \right\} \tag{62}$$

The calculation of the Stokes series has the following steps:

1. Introduce the new coordinate

$$\zeta \equiv k X \tag{63}$$

and the constant phase parameter χ and substitute the expansion

$$\begin{aligned} u \;=\; & \epsilon b_1 \left[\sin(\zeta) + \chi \cos(\zeta)\right] \\ & + \epsilon^2 \left\{ b_{21} \left[\sin(\zeta) + \chi \cos(\zeta)\right] + b_{22} \sin(2\zeta) + a_{22} \cos(2\zeta) \right\} \\ & + \epsilon^3 \left\{ b_{31} \left[\sin(\zeta) + \chi \cos(\zeta)\right] \right. \\ & \left. + b_{32} \sin(2\zeta) + a_{32} \cos(2\zeta) + b_{33} \sin(3\zeta) + a_{33} \cos(3\zeta) \right\} + \dots \end{aligned} \tag{64}$$

into the differential equation to create the "residual function".

2. Collect powers of ϵ.

3. Multiply the residual at $O(\epsilon^n)$ by $\sin(j\zeta), 1 = 2, \dots, n$ and by $\cos(j\zeta), j = 2, \dots, n$ and integrate over ζ from $-\pi$ to π.

4. Solve the resulting equations for the unknown Fourier coefficients at each order and for the wavenumber correction κ_j. (The projections of the residual onto $\cos(\zeta)$ is *redundant*; the coefficients $b_{j1}, j = 2, 3, \dots$ are determined entirely by *matching* to the inner solution.)

Table 5 is a complete program in the computing language Maple for calculating the Stokes' expansion to any order.

The phase parameter χ and the expansion coefficients for the coefficient of $\sin(kX)$, b_1 plus $b_{j1}, j > 1$, are undetermined by the internal dynamics of the outer solution. The reason is that for a given fixed ϵ, a quasi-sinusoidal solution exists for arbitrary phase χ and for arbitrary amplitude a. The amplitude is uniquely fixed by matching to the inner solution, but the phase χ will remain as a free parameter whose significance is discussed in Sec. 9 below.

The Maple output is

$$b_{22} = \frac{2}{3}\chi b_1^2, \qquad a_{22} = \frac{1}{3}\left(\chi^2 - 1\right) b_1^2 \tag{65}$$

$$\kappa_2 = -\frac{1}{2} + \frac{1}{12}\left(\chi^2 + 1\right) b_1^2 \tag{66}$$

$$b_{33} = \frac{3}{16}\,\left(3\,\chi^2 - 1\right)\,b_1^3, \qquad b_{32} = \frac{4}{3}\chi b_1 b_{21} \tag{67}$$

$$a_{32} = \frac{2}{3}\,\left(\chi^2 - 1\right)\,b_1 b_{21}, \qquad a_{33} = \frac{3}{16}\,\chi\,\left(\chi^2 - 3\right)\,b_1^3 \tag{68}$$

$$\kappa_3 = \frac{1}{6}\,b_1\,b_{21}(1+\chi^2) \tag{69}$$

$$b_{44} = \frac{14}{27} b_1^4\,\chi(\chi^2-1), \qquad b_{43} = \frac{9}{16}\,b_1^2\,b_{21}\,\left(3\chi^2 - 1\right) \tag{70}$$

$$b_{42} = \frac{4}{3} b_1 \chi b_{31} + \frac{2}{3}\chi b_{21}^2 + \frac{23}{108}\,b_1^4 \chi\,\left(\chi^2+1\right) - \frac{10}{3}\chi b_1^2 \tag{71}$$

$$a_{44} = \frac{7}{54}\,b_1^4\,\left(\chi^4 - 6\chi^2 + 1\right), \qquad a_{43} = \frac{9}{16}\chi\,b_1^2\,b_{21}\,\left(\chi^2 - 3\right) \tag{72}$$

$$a_{42} = \frac{2}{3} b_1\,\left(\chi^2-1\right) b_{31} + \frac{1}{3}\left(\chi^2-1\right)\,b_{21}^2 + \frac{5}{3}\left(1-\chi^2\right)\,b_1^2 + \frac{23}{216}\,\left(\chi^4-1\right)\,b_1^4 \tag{73}$$

The inner limit of the outer solution is obtained by expanding the Stokes series for small values of the outer coordinate $\xi \equiv \epsilon X$ as defined earlier:

$$u^{(outer)} \approx \sum_{J=1}^{n} \epsilon^J \sum_{K=0}^{\infty} q_{JK}\,\xi^K, \qquad \xi << 1 \tag{74}$$

where the necessary Maple statements have been appended to the table. We find, listing only those coefficients needed for a third order match,

$$q_{10} = \chi\,b_1, \qquad q_{11} = b_1, \qquad q_{12} = -(1/2)\chi\,b_1 \tag{75}$$

$$q_{20} = \frac{1}{3}\,\left(\chi^2-1\right)\,b_1^2 + \chi\,b_{21}, \qquad q_{21} = \frac{4}{3}\chi\,b_1^2 + \,b_{21}, \tag{76}$$

$$q_{30} = \frac{3}{16}\chi\,\left(\chi^2-3\right) b_1^3 + \chi\,b_{31} + \frac{2}{3}\,\left(\chi^2-1\right)\,b_{21}\,b_1 \tag{77}$$

$$q_{31} = -\frac{1}{2}\,b_1 - \frac{23}{48} b_1^3 + \frac{85}{48}\chi^2 b_1^3 + \frac{8}{3}\chi b_1 b_{21} + b_{31} \tag{78}$$

Although we have listed the fourth order outer solution to emphasize the simplicity of the high order outer approximation compared to the not-explicitly-known-beyond-second-order inner solution, the third order outer solution is all that is needed to completely determine via matching all the unknowns in the third order inner approximation.

8 Matching: Solutions

The matching of the inner and outer approximations gives the following formulas for the unknowns. The square brackets give the coefficients of the inner and outer power series whose matching yields the solution for that unknown.

$$b_1 = -6 \qquad [p_{21} = q_{11}] \tag{79}$$

$$\Lambda_1 = 6\,\chi \qquad [p_{10} = q_{10}] \tag{80}$$

$$b_{21} = -30\,\chi \qquad [p_{31} = q_{21}] \tag{81}$$

$$\Lambda_2 = 12(1 + \log(2)) + 36\chi^2 \qquad [p_{20} = q_{20}] \tag{82}$$

$$b_{31} = -66.630399 - \frac{249}{2}\,\chi^2 \qquad [p_{41} = q_{31}] \tag{83}$$

$$\Lambda_3 = 143.130399\,\chi + 153\,\chi^3 \qquad [p_{30} = q_{30}] \tag{84}$$

The phase factor χ, which controls the relative strength of the cosine and sine functions in the outer solution, is still undetermined. We explain its role and determination in the next section.

Table 5: Stokes (Outer Solution) Maple program

```
u:=epsilon* b1*(sin(zeta) + chi*cos(zeta)); ktilde:= 1; maxorder:=4;
for jorder from 2 by 1 to maxorder do # Begin loop over order
ktilde:=ktilde + kappa.(jorder-1) * epsilon**(jorder-1); k:=ktilde*epsilon;
u:= u + epsilon**jorder * b.jorder.1 *(sin(zeta) + chi*cos(zeta));
for j from 2 by 1 to jorder do
u:= u + epsilon**jorder * (b.jorder.j * sin(j*zeta) + a.jorder.j * cos(j*zeta)); od:
residual:= (k**4*diff(u,zeta,zeta,zeta,zeta) + (u-1)*k**2 * diff(u,zeta,zeta)
+ k**2*(diff(u,zeta))**2 - epsilon*epsilon*u) / (epsilon*epsilon);
# Pick off O(epsilon**jorder) part of the residual
residual_thisorder:= coeff(collect(simplify(residual),epsilon),epsilon,jorder);
# Compute correction to the wavenumber, ktilde
eq0:= int(sin(zeta)*residual_thisorder,zeta=-Pi..Pi);
if (coeff(eq0,kappa.(jorder-1),1) = 0) then kappa.(jorder-1):=0;
else kappa.(jorder-1):= simplify(solve(eq0,kappa.(jorder-1))); fi;
setofequations:= {   }; setofunknowns:={   };
        for j from 2 by 1 to jorder do
        eq.j:= int(sin(j*zeta)*residual_thisorder,zeta=-Pi..Pi);
        eq.(j+jorder):= int(cos(j*zeta)*residual_thisorder,zeta=-Pi..Pi);
        setofequations:= setofequations union {eq.j, eq.(j+jorder) };
        setofunknowns:= setofunknowns union {b.jorder.j, a.jorder.j };
        od: # end of j loop
solutionforcoeffs:= solve(setofequations,setofunknowns); assign(solutionforcoeffs);
od: # end of jorder loop
```

```
# Next, expand outer solution as power series in outer coordinate ξ ≡ εX
nmax:=4;
uouter_smallxi:= series( simplify(subs(zeta=k*xi/epsilon,u)),xi,nmax);
for m from 0 by 1 to nmax do
uuu.m:= coeff(uouter_smallxi,xi,m); # coefficients of power series in xi
for j from 1 by 1 to nmax do
q.j.m := coeff(collect(uuu.m,epsilon),epsilon,j); # compute q_jm
od: od: # end of loops in j, m
```

9 Minimum Radiation and Resonance

On the infinite interval, the phase parameter χ is undetermined. This reflects the freedom, ubiquitous in the theory of nonlocal solitary waves, to add an arbitrary small multiple of an eigenfunction to a solution to obtain an another solution. (The eigenfunction is a mode of zero eigenvalue for the fourth order ordinary equation, linearized with respect to a nonlocal solitary wave; in the perturbation theory, the eigenfunction is equal to $\mathcal{E}$ (u_1) in the inner region and matches to $\cos(kX)$ in the outer region.)

By differentiating the amplitude of the fundamental, suitably expanded as a power series in ϵ, with respect to χ and then expanding the root in ϵ, too, one finds that this is minimized when

$$\chi \approx -5\epsilon + 13.025332\epsilon^3 + O(\epsilon^4) \tag{85}$$

(By the "amplitude of the fundamental", we mean the coefficient of $\sin(k[X+\Phi])$ when $\sin(kX)$ and $\cos(kX)$ are combined into a single trignometric function via a trigonometric identity.)

However, the matched asymptotic series applies equally well when boundary conditions of spatial periodicity are imposed. In this case, however, χ is no longer a free parameter, but instead must assume a unique value so that the wave is periodic with a given spatial period P in X.

Let us define the slope of the wave at the end of the periodicity interval to be s, that is,

$$u_X(P/2) \equiv s \tag{86}$$

The symmetry of the wave with respect to $X = 0$ implies that its first derivative is antisymmetric with respect to X and therefore

$$u_X(-P/2) = -s \tag{87}$$

However, the periodicity requirement that $u(X + P) = u(X)$ for all X demands

$$u_X(-P/2) = u_X(P/2) = s \tag{88}$$

The only way that the slope at $X = -P/2$ can be both s and $-s$, and thus satisfy the twin constraints of periodicity and symmetry, is if $s = 0$. Thus,

$$u_X(\pm P/2) = 0 \tag{89}$$

The Stokes expansion can, with a shift of coordinates, be written as a cosine series as noted earlier. The boundary condition can be interpreted as the requirement that the peaks of the cosines coincide with $X = P/2$. It is sufficient to choose χ so that the fundamental, which is proportional to $\sin(kX)+\chi\cos(kX)$, has zero slope at the boundary point because then all the higher harmonics will, too. This constraint on the fundamental gives

$$\chi = \cot(kP/2) \tag{90}$$

Unfortunately, the wavenumber k implicitly depends upon χ through the higher order corrections in ϵ. It is therefore necessary to expand χ as a series in powers of ϵ to solve Eq. 90. It is convenient to introduce the "period parameter"

$$\nu \equiv P\epsilon/(2\pi) \tag{91}$$

since P is typically $O(1/\epsilon)$ or larger in applications. One finds

$$\chi = \cot(\pi\nu) - \pi\nu \left(\frac{5}{2} + \frac{11}{2}\cot^2(\pi\nu) + 3\cot^4(\pi\nu) \right) \epsilon^2 + O(\epsilon^3) \tag{92}$$

It is easiest to understand the implications of the phase parameter by restricting ourselves to the limit $\epsilon \to 0$ and ignoring the higher-order-in-ϵ corrections. Then the limit of the oscillations in the outer solution is minimized when $\chi = 0$, which requires

$$P = \frac{(2m+1)\,\pi}{\epsilon}, \qquad m = \text{integer} \qquad \text{Minimum Radiation Condition at Lowest Order} \tag{93}$$

or in other words, the period parameter ν must be halfway between an integer. Interlacing these periods of minimum outer solution are choices of spatial period P such that $\chi = \infty$:

$$P = \frac{2m\,\pi}{\epsilon}, \qquad m = \text{integer} \qquad \text{Resonance Condition} \tag{94}$$

or in other words, the outer solution is huge as the period parameter ν tends to an integer.

This is not surprising because when ν is an integer, an integral number of wavelengths of $\cos(kX)$ will fit on the interval $X \in [-P/2, P/2]$. The amplitude of the eigenfunction, which is equal to $\cos(kX)$ over most of the interval, can therefore be made arbitrarily large without violating the boundary condition of spatial periodicity.

Of course, the matched asymptotics is not justified when χ is large because then the underlying premise that the outer solution is small is no longer true.

10 Numerical Methods

The accuracy of perturbative analysis can be tested by direct comparison with Fourier pseudospectral solutions. The zero mean condition is implemented by omitting the constant in the Fourier series; the condition of symmetry is imposed (and the translational eigenfunction suppressed) by using a basis of cosines only.

In brief, the solution is expanded as

$$u(X) \approx \sum_{n=1}^{N} a_n \, cos(2\pi n X/P) \tag{95}$$

where N is the truncation of the Fourier series and P is the spatial period. This is substituted into the differential equation to define the "residual function" $R(X; a_1, a_2, \ldots, N)$. Imposing the "collocation" or pseudospectral requirement that $R(x_i; a_1, a_2, \ldots, N) = 0$ at each of N points on an evenly-spaced grid spanning one spatial period converts the differential equation into a system of N algebraic equations in N unknowns, the spectral coefficients $\{a_j\}$. This algebraic system is solved by Newton's iteration.

The details are described at length in [5, 6] and will not be repeated here. One drawback of Newton's iteration is that it requires an initial guess. Perturbation theory and analytical approximations are a powerful source of such initializations. Once a single point on a branch has been found, one can march to other points on the branch by altering a parameter such as ϵ in small steps, using the solution for the previous point as the first guess for its nearest neighbor. Through this "continuation" method, one can trace an entire solution branch far beyond the limits of perturbation theory. Keller's monograph[18] and, more briefly, Appendices C and D of [6] describe how continuation can be generalized to turn around limit points or leap past bifurcation points.

11 Bifurcation

As ϵ increases, the height of the small, large X oscillations increases, too. To satisfy the differential equation, these peaks must become narrower, and thus more strongly curved, as their amplitude increases. This suggests that for sufficiently large ϵ, the secondary peaks, described for small ϵ by the Stokes expansion, will eventually become as tall and narrow as the core peaks. What happens then? The obvious scenario is that the modes with both tall and short peaks bifurcate from the quasi-cnoidal wave, which has all maxima of the same size.

At some points in parameter space, this is exactly what happens as illustrated in Fig. 5.

First, though, an important aside. Because the far field wavenumber k is inversely proportional to ϵ, the number of oscillations per spatial period varies wildly with ϵ for *fixed spatial period*. Indeed, fixed-P-and-variable-ϵ passes from resonance to minimum outer solution and back again. To understand the physics, it is almost essential to pursue a different ray in parameter space: variable ϵ with the spatial period P varying *inversely* with ϵ. This variable-P convention is used in Fig. 5 and all that follow as well as in our companion paper[8].

One finds that the solution illustrated in Fig. 5, which is well-described by matched asymptotics for small ϵ, bifurcates from the quasi-cnoidal wave at $\epsilon \approx 0.1418$. Fig. 6 shows how the heights of the primary and second peaks vary with ϵ. Beyond the bifurcation point, $\epsilon_{bif} = 0.1418$, there exists only the quasi-cnoidal mode. For $\epsilon < \epsilon_{bif}$, there are three modes. One is the quasi-cnoidal mode, the second is the one-tall/one-short peak-on-each-period mode which is illustrated in the figures, and the third mode is the same as the second but with a phase shift of $P/2$ so that the taller peaks are at $X = \pm P/2, 3P/2, 5P/2$, etc. The third mode obviously bifurcates at the same point as the second since these mode are identical except for a translation in space.

The bifurcation point can be computed directly by noting that it occurs when the Jacobian matrix of the Newton's iteration becomes singular. This matrix can be obtained directly by linearizing the differential equation with respect to a solution and applying the pseudospectral method to convert the differential equation to a matrix problem. In our case, it is convenient to linearize about the quasi-cnoidal mode. Bifurcation occurs when one of the eigenvalues becomes zero. The corresponding eigenfunction gives the difference between the cnoidal wave and the modes that bifurcate from it. The amplitude of the singular eigenmode in each bifurcating solution is indeterminate from the linearized problem, but can be determined by solving the full nonlinear RMKdV equation, provided ϵ is at least different from ϵ_{bif}.

Fig. 7 shows both the quasi-cnoidal wave (dashed) and the eigenfunction (solid). The crucial point is the features of the eigenfunction are of opposite sign at $X = 0$ and $X = \pm P/2$. This means that adding a small multiple of the eigenmode to the quasi-cnoidal wave will reinforce one set of peaks and reduce the other. Thus, the subharmonic bifurcation of the quasi-cnoidal wave generates modes with twice the spatial period of the quasi-cnoidal wave and

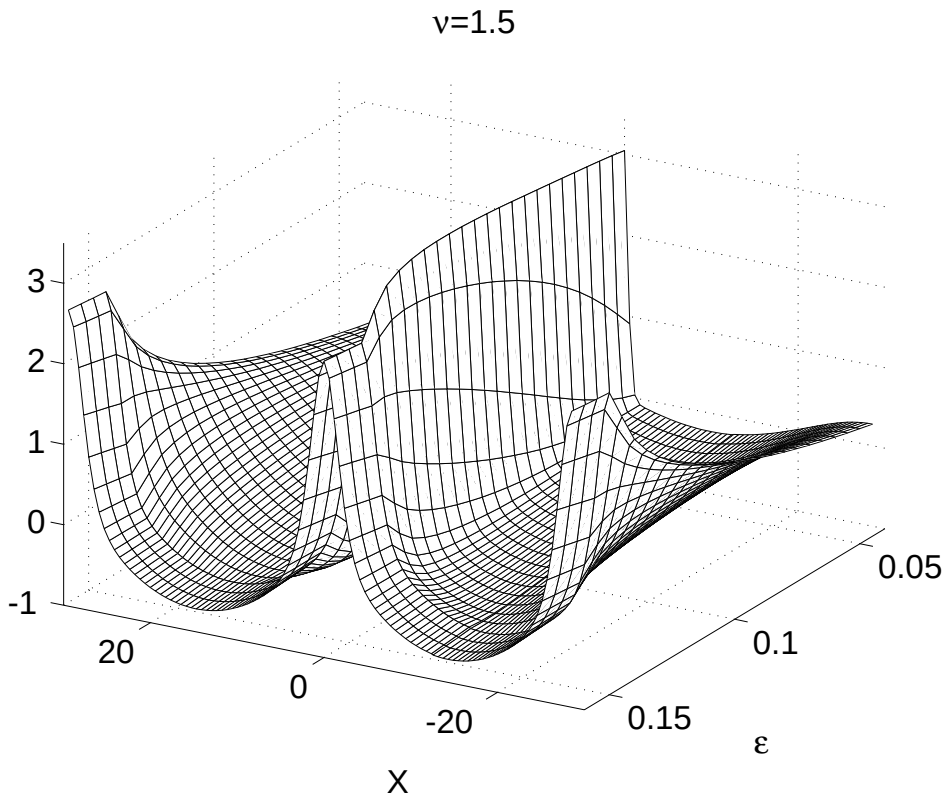

Figure 5: Mesh plot $u(X;\epsilon)$ for various ϵ; the period varies with ϵ so that $P = 3\pi/\epsilon$ for all ϵ, or in other words the "period parameter" ν is fixed at $3/2$.

with local maxima of two different sizes — only slightly different when ϵ is close to the bifurcation point.

When the spatial period is increased for a given ϵ, more complicated modes and bifurcations appear. Fig. 8 shows the four different shapes of modes that are relevant for the slice through parameter space such that

$$P = 3.75\,\frac{\pi}{\epsilon}\,. \tag{96}$$

The top pair of modes are "quasi-cnoidal" in the sense that all their peaks, for a given period and rotation parameter ϵ, are identical. Each of the lower modes has maxima of two different sizes and bifurcates from the quasi-cnoidal species illustrated just above it.

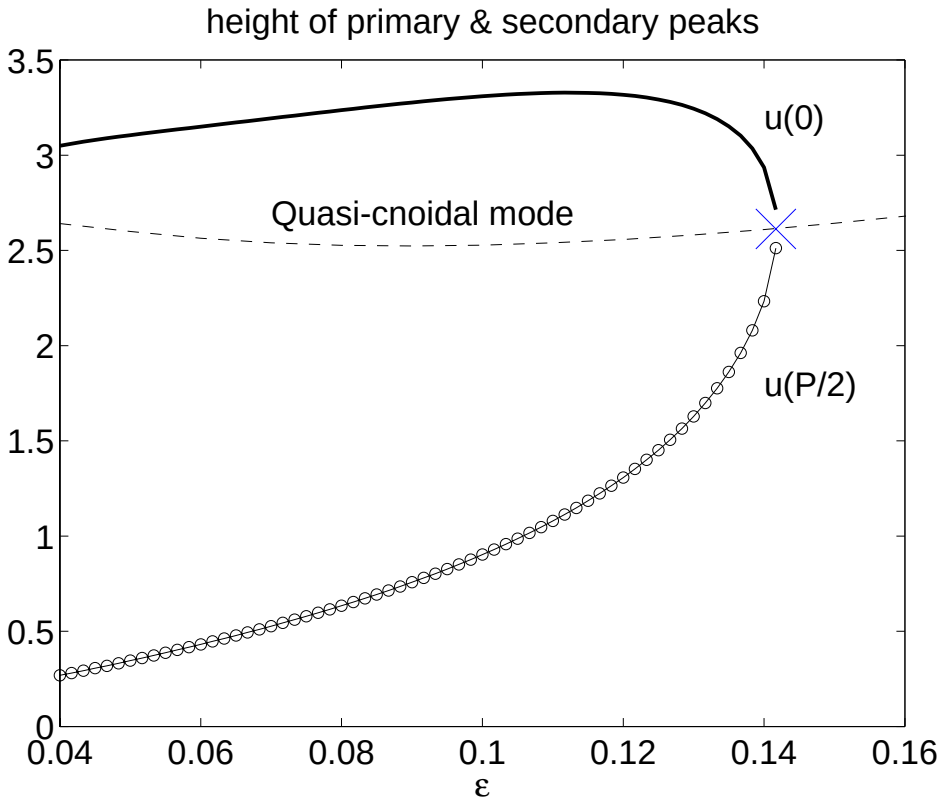

Figure 6: Same case as the previous figure. The upper curve (thick solid) is $u(X = 0)$ for the mode with one tall peak at the origin and a shorter local maximum at $X = P/2$; the lower curve with circles is the amplitude of this smaller peak. The thin solid line in the middle is the height of the peaks for quasi-cnoidal wave, which are all of identical size for a given ϵ. The upper and lower curves can alternatively be interpreted as the heights of the tall and short peaks of the mode which is the translation of the first mode so that the tall peak is at $X = P/2$ and the smaller maximum at the origin. The two modes with unequal heights do not exist beyond the bifurcation point at $\epsilon = \epsilon_{bif}$ where only the quasi-cnoidal wave (with all equal peaks) survives. The bifurcation point is marked with a large "X".

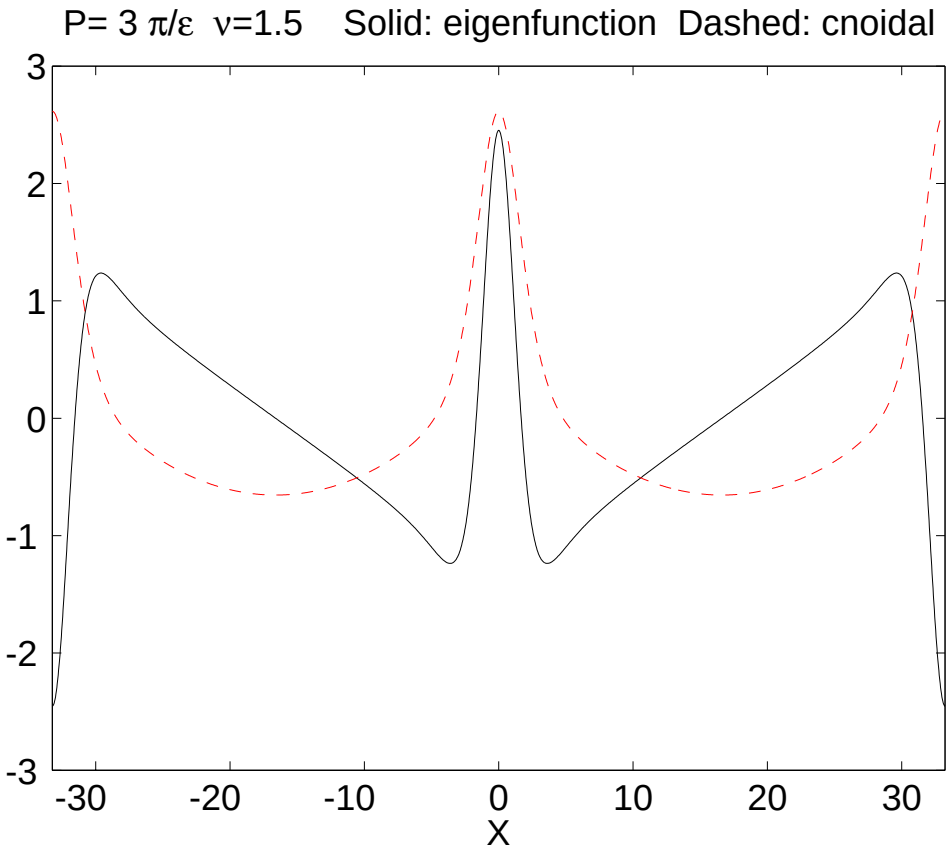

Figure 7: The subharmonic eigenfunction has period $P = 3\pi/\epsilon$. The Stokes wave from which it bifurcates has a period equal to ONE-HALF of the eigenfunction.

Fig. 9 shows the bifurcation points and limit points on a graph of the local maxima of u for each mode. The [1/1] mode (dashed curve) has one maxima equal to three and the other proportional to ϵ in the limit $\epsilon \to 0$ as illustrated in Fig. 10. As ϵ increases, the tall peak (upper half of dashed curve) becomes shorter while the lower peak (bottom half of dashed curve) becomes taller. At the bifurcation point (solid disk), $\epsilon \approx 0.053$, the two peaks have become equal and the mode merges with the quasi-cnoidal wave that has two identical peaks on each period for all ϵ. This bifurcation is very similar to that which occurs for smaller spatial period as illustrated earlier in Fig. 6.

The [2/1] mode (solid) has two identical maxima equal to three and a small peak proportional to ϵ when ϵ is very small. As ϵ increases, the height of the pair of tall peaks first increases, then decreases to a limit point at about $\epsilon \approx 0.108$. Rounding the limit point and thus marching back towards smaller ϵ, the height of the tall peaks continues to decreases until the mode merges with the quasi-cnoidal wave with three identical maxima on each interval of length $3.75\pi/\epsilon$ at $\epsilon \approx 0.0778$. Similarly, the height of short peak rises, rounds the limit point, and finally equals that of the pair of taller peaks at the bifurcation point (solid disk). The limit point is marked on the graphs of both the taller and shorter maxima by the triangles at $\epsilon = 0.108$.

Fig. 12 illustrates the eigenfunction at $\epsilon = 0.078$ where the [2/1] mode bifurcates as third-subharmonic from the quasi-cnoidal wave. The eigenfunction is quite different from that of the half-harmonic bifurcation: here, the central peak of the eigenfunction is very small so that one peak is little altered by adding a small multiple of the eigenfunction to the quasi-cnoidal wave. The other features of the eigenfunction are a pair of structures that each consist of a crest and an equal-but-opposite valley adjacent to one another with the center of each structure aligned with a crest of the quasi-cnoidal wave. These peak-and-valley structures resemble the X-derivative of a peak of the quasi-cnoidal wave — they are sech-tanh-like in the same way that the peaks of the quasi-cnoidal wave are sech-squared-like — and serve to *translate* the peaks of the quasi-cnoidal wave.

The [2/1] mode can be described by the matched asymptotic expansions derived earlier, but only with a little additional analysis which is given in the next section.

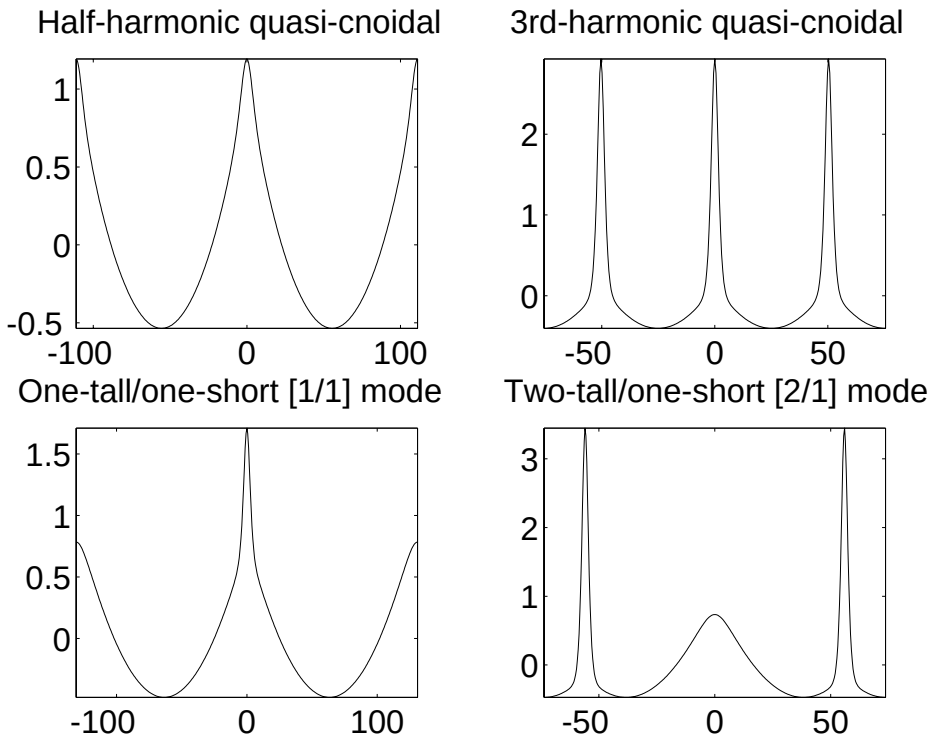

Figure 8: Four species of steadily-translating waves when $P = 3.75\pi/\epsilon$. The lower pair of modes have maxima of two different sizes. The lower left mode is called the "[1/1]" mode because it has one tall and one short peak on each spatial period. It bifurcates from the quasi-cnoidal mode above it (the "half-harmonic") at $\epsilon \approx 0.053$. Similarly the lower right wave is the "[2/1]"' mode because it has two tall, narrow peaks and one short, broad peak on each spatial period. It bifurcates from the quasi-cnoidal wave in the top right ("third-subharmonic") at $\epsilon \approx 0.0778$.

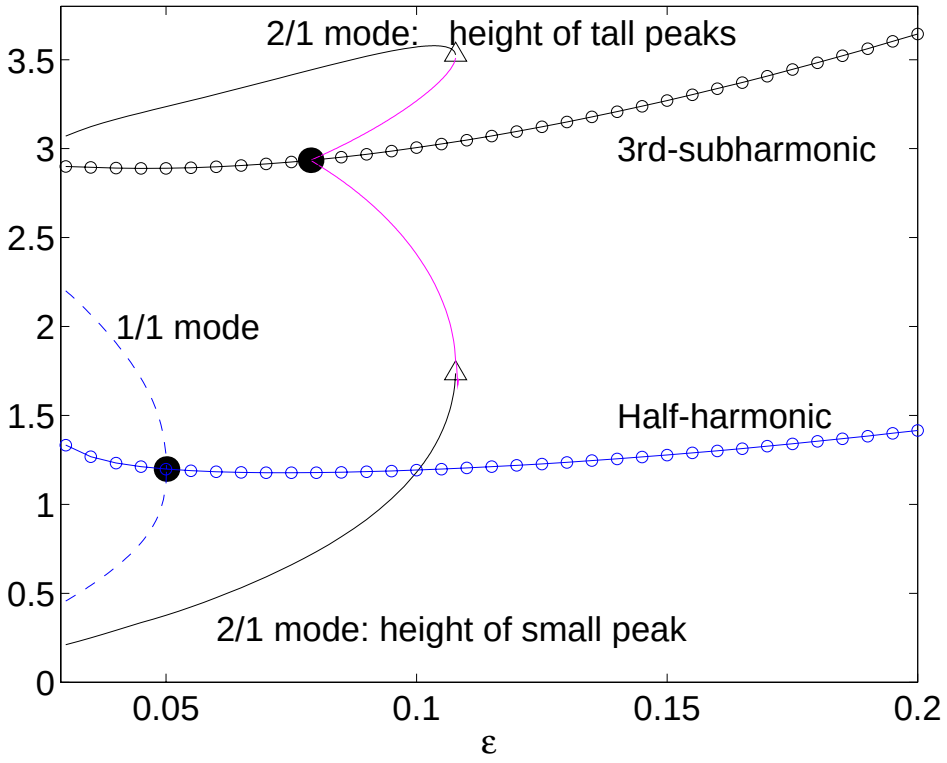

Figure 9: Bifurcation diagram for $P = 3.75\pi/\epsilon$, plotting the local maxima in u for each mode as ϵ varies on the interval $\epsilon \in [0.03, 0.2]$. The dotted curves are the maxima-in-X of $u(X;\epsilon)$ for the quasi-cnoidal waves; these by definition are modes for which all the peaks at a given ϵ and spatial period are identical. The dashed curve shows the height of the tall peak and of the short peak for the pair of modes that have one tall maxima and one smaller maxima on each spatial period. (These two "[1/1]" modes are identical except for a spatial translation by $P/2$.) These modes exist only for $\epsilon < \epsilon_{bif}$ where the bifurcation point, denoted by the black disk, is at $\epsilon_{bif} \approx 0.053$. The one-tall/one-short modes bifurcate from the quasi-cnoidal wave which has two identical peaks on each interval of length P; this quasi-cnoidal wave is a "half-harmonic" in the sense that its spatial period is $P/2$, half that of the "[1/1]" modes that bifurcate from it. The mode with two tall peaks and one short, broad maxima on each period ("[2/1]") bifurcates from a quasi-cnoidal wave, too, but one whose period is $P/3$. The [2/1] mode also has a limit point at $\epsilon = 0.108$ which is marked by large triangles at the limiting heights of the tall and short peaks.

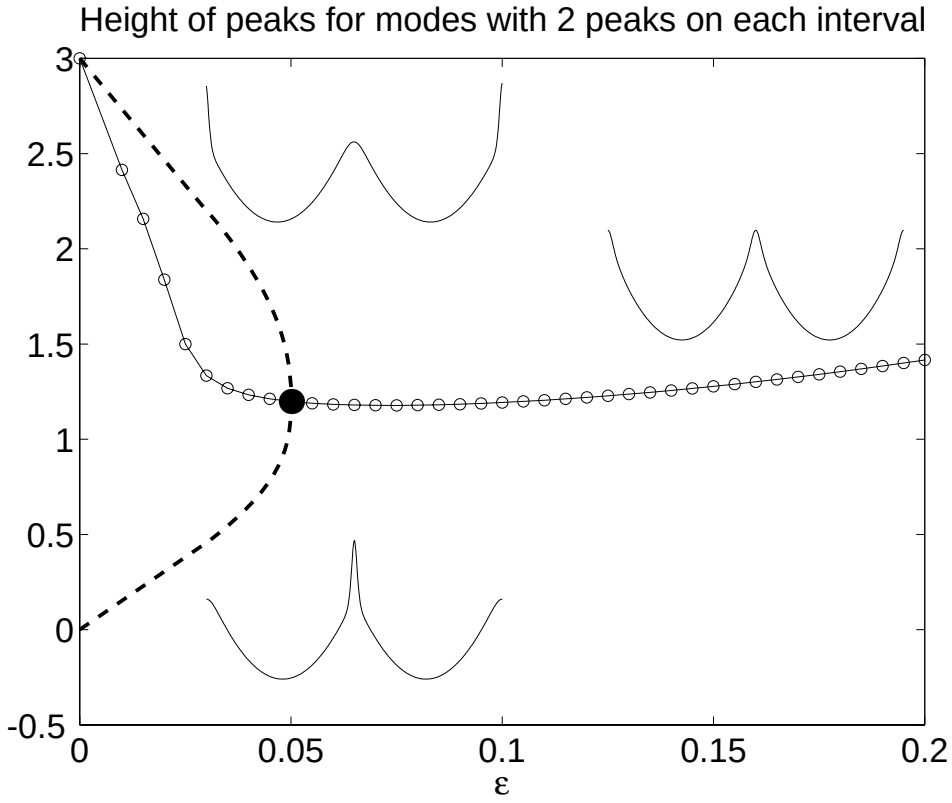

Figure 10: Same as the previous diagram, but showing only the modes with two maxima on each spatial period. The curve with open circles shows the height of the pair of peaks for the quasi-cnoidal wave; its shape is depicted in the rightmost insert graph. The upper dashed curve shows the height of the larger maxima for the [1/1] mode while the lower dashed curve is the height of the short, broad peak for the same mode. The point where the [1/1] mode bifurcates from the quasi-cnoidal wave is marked by the filled disk at $\epsilon = 0.053$. There are actually two [1/1] modes which differ only by a translation by half the period or equivalently, differ only in that one species has the tall peak at the origin (bottom insert graph) whereas the other has the tall peaks at $X = \pm P/2$.

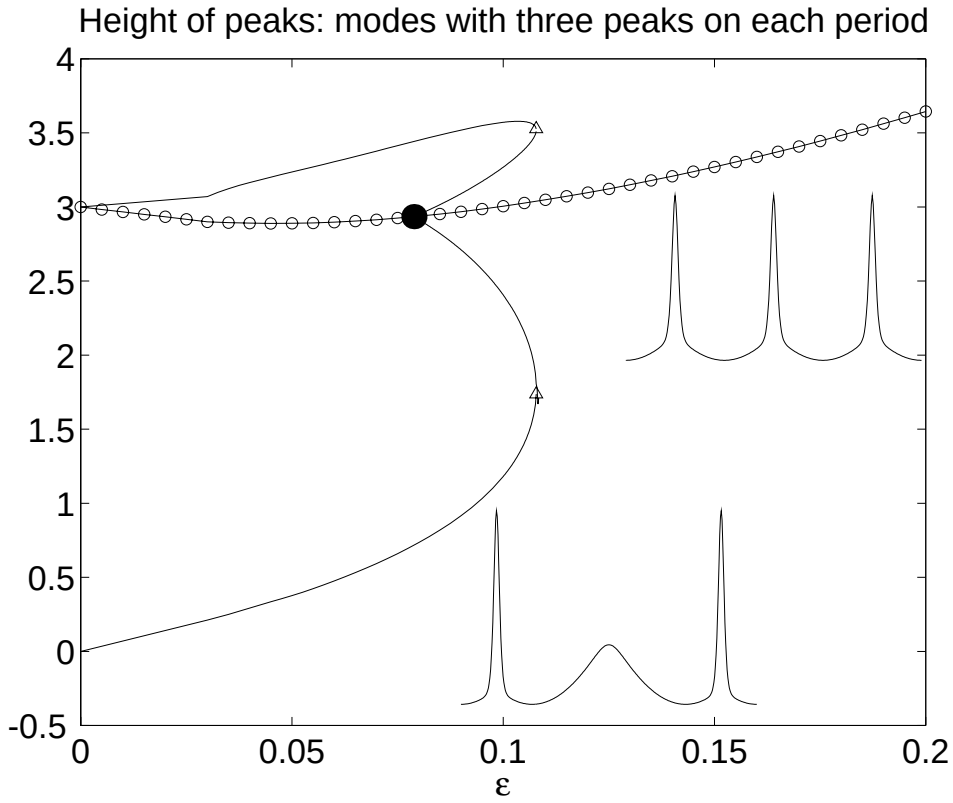

Figure 11: Same as the previous diagram, but for the modes with three maxima on each spatial period. The curve with open circles shows the height of the trio of peaks for the quasi-cnoidal wave; its shape is depicted in the rightmost insert graph. The thin curves show the heights of the tall peaks (curve above the quasi-cnoidal peaks) and short peak (curve below the disk) for the mode with two tall peaks and one short peak on each period.

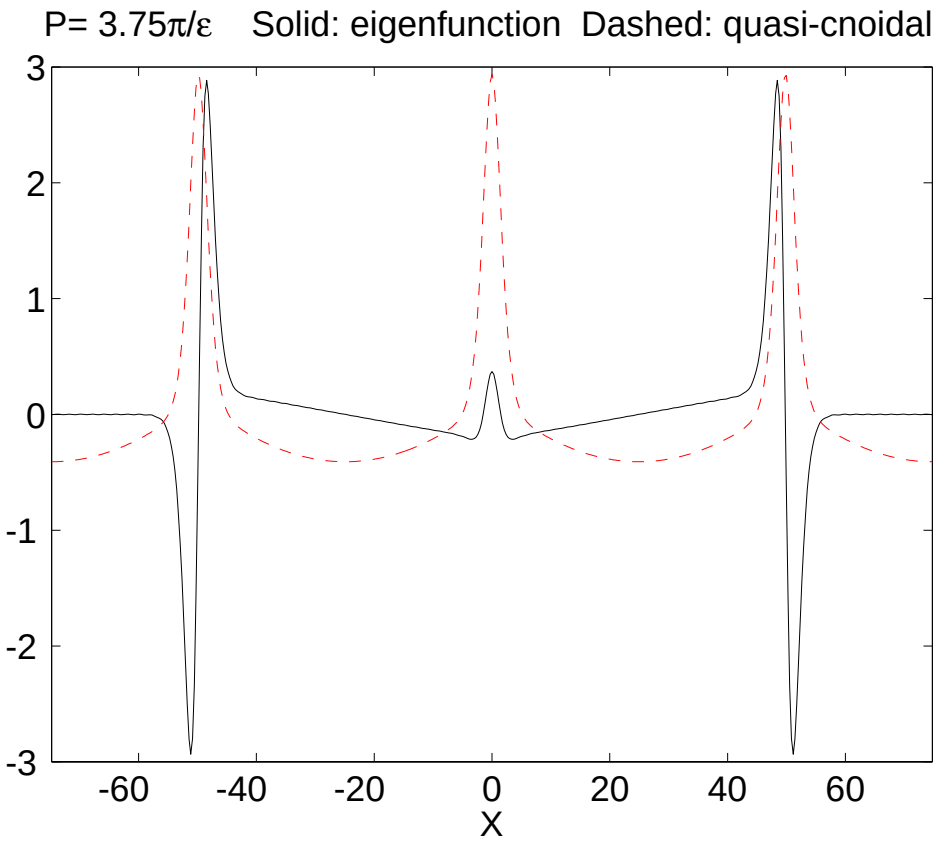

Figure 12: The subharmonic eigenfunction (solid curve) has period $P = 3.75\pi/\epsilon$, three times that of the quasi-cnoidal wave from which it bifurcates at $\epsilon \approx 0.078$.

12 Asymptotic Approximation to Modes with Two Sech-Squared Peaks on Each Period for Small ϵ

Key assumption: each tall peak is symmetric with respect to its own center. This is a strong assumption because we have no theorem to rule out asymmetry.

Define $P_2/2$ to be the distance from the right tall peak to the edge of the periodicity interval at $X = P/2$. Define $P_1/2$ to be the distance from the right core peak to $X = 0$. From these definitions, it follows immediately that

$$P_1 + P_2 = P\,. \tag{97}$$

If the pieces are to blend together, we have zero slope at both $X = 0$, the valley between the left and right tall peaks, and also at $X = P/2$. Because of our symmetry assumption, it follows that the phase factor χ of the outer solution is the same both to the left and to the right of the tall peak and therefore does not need a subscript. The zero slope condition then requires

$$\chi = \cot(kP_1/2) = \cot(kP_2/2)\,. \tag{98}$$

This implies to all orders in the matched asymptotics that

$$kP_2/2 = kP_1/2 + n\pi \tag{99}$$

where n is an integer. In other words, using $P_1 = P - P_2$,

$$\boxed{P_2 = \tfrac{P}{2} + n\pi\tfrac{1}{k(\epsilon)}} \qquad \boxed{P_1 = \tfrac{P}{2} - n\pi\tfrac{1}{k(\epsilon)}} \tag{100}$$

Unfortunately, k depends on the phase χ, and χ in turn depends on P_1 and P_2, which determine k. It is necessary to simultaneously solve the trio of equations

$$\chi = \cot(kP_2/2) \tag{101}$$

$$P_2 = \frac{P}{2} + n\pi\frac{1}{k(\epsilon)} \tag{102}$$

$$k \approx \epsilon + \left\{\frac{5}{2} + 3\chi^2\right\}\epsilon^3 + \left\{30\chi + 30\chi^3\right\}\epsilon^4 \tag{103}$$

Define the auxiliary parameter

$$\mu = \frac{\pi}{2}\,(\nu + n) \tag{104}$$

Then

$$\chi \approx \cot(\mu) + \left(-\frac{1}{2}\mu + \frac{1}{4}\pi n\right)\left\{\left(5 + \cos^2(\mu)\right)\frac{1}{\sin^4(\mu)}\right\}\epsilon^2 + 15(-2\mu + \pi n)\cot(\mu)\frac{1}{\sin^4(\mu)}\epsilon^3 + O\left(\epsilon^4\right) \tag{105}$$

Once χ is known, we can easily substitute this formula to compute k and then P_2.

Fig. 13 shows that the matched asympotics approximation to the [2/1] mode is very accurate.

13 Prospectus

Much is now known about the Rotation-Modified Korteweg-deVries equation, but many issues are still unresolved. It is likely that there are modes with an arbitrary number of tall peaks and short maxima on each interval, and a corresponding diversity of bifurcations and limit points. The stability of the modes described here and of the many undiscovered modes is not known. There have been some limited studies of the initial value problem; Grimshaw, He and Ostrovsky[15] have observed the radiative decay of a solitary wave, followed by the spontaneous refocusing of the coherent structure. It is possible that more exotic behavior remains undiscovered.

On the other hand, we have extended the matched asymptotic analysis to fourth order without finding any novelties; it seems that the perturbation theory for small ϵ is straightforward. However, the numerical problems that arose in matched asymptotics, here and in many similar problems, required novel spectral methods for solutions with polynomial-growth-in-x on an unbounded spatial domain[7]. Furthermore, the new parabolic mode of the quasi-cnoidal wave, discussed in our companion article[8], has not yet received a satisfactory analysis.

The addition of a single undifferentiated term, multiplied by the square of a small parameter ϵ, would not seem to produce profound alterations to the well-understood behavior of KdV waves. Our article and other work referenced above shows that just the opposite is true: the perturbation that alters the KdV equation into the RMKdV equation introduces a plethora of new modes and new behavior.

Acknowledgments

This work was supported by National Science Foundation through OCE9521133. Dr. Chen is grateful for a three-year graduate fellowship provided by the Department of Education, Taiwan, R. O. C.

References

[1] M. Abramowitz and I. A. Stegun, *Handbook of Mathematical Functions*, Dover, New York, 1965.

[2] E. Benilov, *The generation of radiating waves in a singularly perturbed Korteweg-deVries equation*, Studies in Applied Mathematics, 87 (1992), pp. 1–14.

[3] J. P. Boyd, *Solitons from sine waves: analytical and numerical methods for non-integrable solitary and cnoidal waves*, Physica D, 21 (1986), pp. 227–246.

[4] ——, *Chebyshev and Fourier Spectral Methods*, Springer-Verlag, New York, 1989. 792 pp.

[5] ——, *Weakly Nonlocal Solitary Waves and Beyond-All-Orders Asymptotics: Generalized Solitons and Hyperasymptotic Perturbation Theory*, vol. 442 of Mathematics and Its Applications, Kluwer, Amsterdam, 1998. 608 pp.

[6] ——, *Chebyshev and Fourier Spectral Methods*, Dover, New York, 2000.

[7] ——, *Rational Chebyshev spectral methods for unbounded solutions on an infinite interval using polynomial-growth special basis functions*, Appl. Numer. Comput., (2000).

[8] J. P. Boyd and G.-Y. Chen, *Five regimes of the quasi-cnoidal, steadily-translating waves of the Rotation-Modified Korteweg-deVries ('Ostrovsky') equation*, Wave Motion, (2000).

[9] G.-Y. Chen, *Application of Weak Nonlinearity in Ocean Waves*, Ph. D. dissertation, University of Michigan, Department of Atmospheric, Oceanic and Space Science, July 1998.

[10] V. M. Galkin and Y. A. Stepanyants, *On the existence of stationary solitary waves in a rotating fluid*, J. Appl. Math. Mech., 55 (1991), pp. 939–943.

[11] O. A. Gilman, R. Grimshaw, and Y. A. Stepanyants, *Approximate analytical and numerical solutions of the stationary Ostrovsky equation*, Stud. Appl. Math., 95 (1995), pp. 115–126.

[12] ——, *Dynamics of internal solitary waves in a rotating fluid*, Dyn. Atmos. Oceans, 23 (1996), pp. 403–411.

[13] R. Grimshaw, L. A. Ostrovsky, V. I. Shrira, and Y. A. Stepanyants, *Nonlinear surface and internal gravity waves in a rotating ocean*, Surveys in Geophysics, 19 (1998), pp. 289–338.

[14] R. H. J. Grimshaw, *Evolution equations for weakly nonlinear, long internal waves in a rotating fluid*, Stud. Appl. Math., 73 (1985), pp. 1–33.

[15] R. H. J. Grimshaw, J.-M. He, and L. A. Ostrovsky, *Terminal damping of a solitary wave due to radiation in rotational systems.*, Stud. Appl. Math., 101 (1998), pp. 197–210.

[16] S. E. Haupt and J. P. Boyd, *Modeling nonlinear resonance: A modification to Stokes' perturbation expansion*, Wave Motion, 10 (1988), pp. 83–98.

[17] J. K. Hunter, *Numerical solutions of some nonlinear dispersive wave equations*, Lectures in Applied Mathematics, 26 (1990), pp. 301–316.

[18] H. B. Keller, *Numerical Methods for Two-Point Boundary-Value Problems*, Dover, New York, 1992.

[19] A. I. Leonov, *The effect of Earth rotation in the propagation of weak nonlinear surface and internal long ocean waves*, Annals of the New York Academy of Sciences, 373 (1981), pp. 150–159.

[20] L. Lewin, *Dilogarithms and Associated Functions*, Macdonald, London, 1958.

[21] L. A. Ostrovsky, *Nonlinear internal waves in a rotation ocean*, Oceanology, 18 (1978), pp. 181–191.

[22] L. A. Ostrovsky and Y. A. Stepanyants, *Nonlinear surface and internal waves in rotating fluids*, in Nonlinear Waves 3, A. V. Gaponov-Grekhov, M. I. Rabinovich, and J. Engelbrecht, eds., New York, 1990, Springer, pp. 106–128.

[23] L. G. Redekopp, *Nonlinear internal waves in geophysics: Long internal waves*, Lectures in Applied Mathematics, 20 (1990), pp. 59–78.

[24] M. Van Dyke,*Perturbation Methods in Fluid Mechanics*, 2d. ed., Parabolic Press, Stanford, California, 1975.

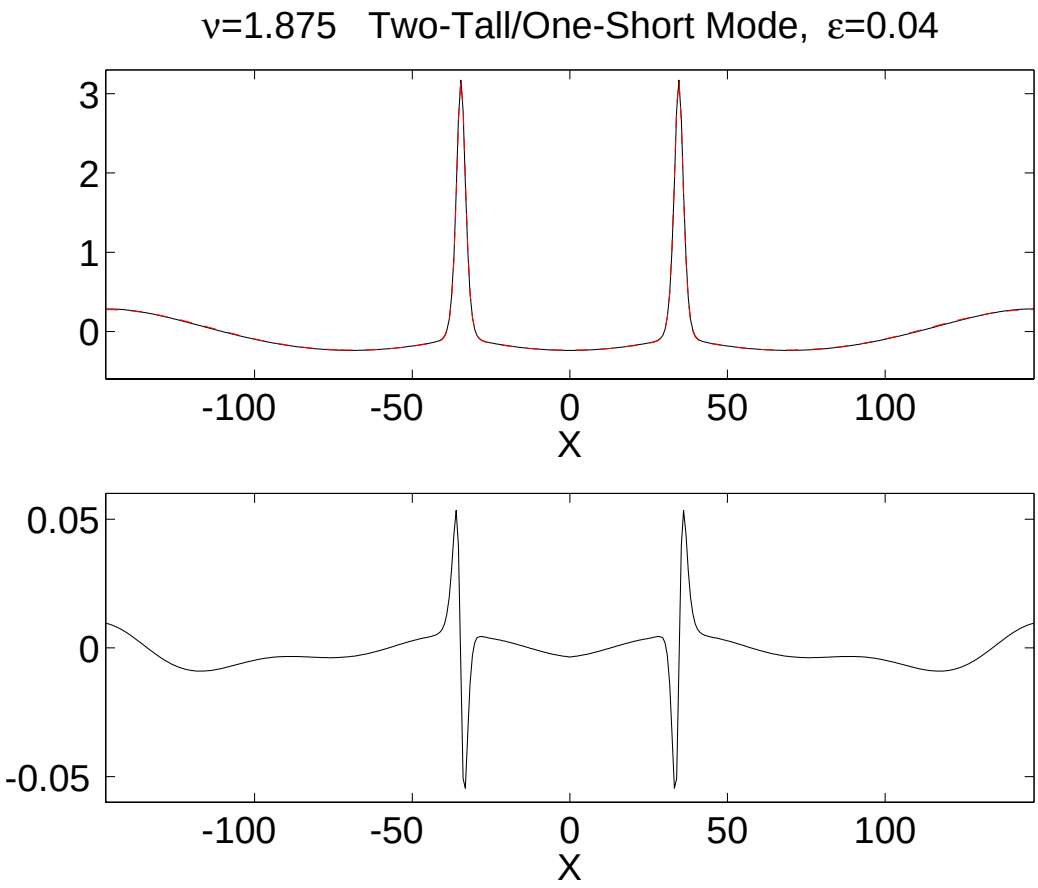

Figure 13: $\nu = 1.875 \leftrightarrow P = 3.75\pi/\epsilon$. Top compares the numerical and two-term composite asympotic approximation to the mode with two tall and one short peak on each interval. (There are really two graphs, solid and dashed, respectively, but these are almost indistinguishable.) The lower panel shows the absolute error. The maximum of the absolute error is 1.7% of the maximum of u. However, this number is misleadingly large. The dipole-structure of the error near the two tall peaks has roughly the shape of the X-derivative of $3\text{sech}^2(X/2)$. This implies that the error could be greatly reduced or even eliminated by slightly moving the location of the two tall peaks.